aeromet

RADIO FREQUENCY HAZARD MONITORING - USAKA

FINAL REPORT

SBIR Topic A90-444

For the Period February 21, 1991 through October 21, 1991

Submitted to

U.S. ARMY STRATEGIC DEFENSE COMMAND
ATTN: CSSD-AT-E/John F. Phillips
P.O. Box 1500
Huntsville, AL 35807-3801

Contract No. DASG60-91-C-0027
CDRL A002

Effective Date: 21 February 1991
Expiration Date: 21 August 1991 extended to 21 October 1991

AEROMET/TUL 9110151

Submitted by

David H. Brown, Principal Investigator/Project Manager
918-299-2621 or DSN 956-5546

Aeromet, Inc.
P.O. Box 701767
Tulsa, OK 74170-1767

November 19, 1991

aeromet inc.

P.O. BOX 701767
TULSA, OK 74170-1767
918-299-2621

SECURITY CLASSIFICATION OF THIS PAGE

REPORT DOCUMENTATION PAGE

Form Approved
OMB No. 0704-0188

1a. REPORT SECURITY CLASSIFICATION Unclassified	1b. RESTRICTIVE MARKINGS See clause H23
2a. SECURITY CLASSIFICATION AUTHORITY U.S. Army Strategic Defense Command	3. DISTRIBUTION/AVAILABILITY OF REPORT Unclassified/Unlimited
2b. DECLASSIFICATION/DOWNGRADING SCHEDULE N/A	
4. PERFORMING ORGANIZATION REPORT NUMBER(S) AEROMET/TUL 9110151	5. MONITORING ORGANIZATION REPORT NUMBER(S) To be assigned.
6a. NAME OF PERFORMING ORGANIZATION Aeromet, Inc. — 6b. OFFICE SYMBOL (If applicable)	7a. NAME OF MONITORING ORGANIZATION U.S. Army Strategic Defense Command
6c. ADDRESS (City, State, and ZIP Code) P.O. Box 701767 Tulsa, OK 74170-1767	7b. ADDRESS (City, State, and ZIP Code) P.O. Box 1500 Huntsville, AL 35807-3801
8a. NAME OF FUNDING/SPONSORING ORGANIZATION U.S. Army Strategic Def. Comm — 8b. OFFICE SYMBOL (If applicable) CSSD-AT-E	9. PROCUREMENT INSTRUMENT IDENTIFICATION NUMBER Contract #DASG60-91-C-0027
8c. ADDRESS (City, State, and ZIP Code) P.O. Box 1500 Huntsville, AL 35807-3801	10. SOURCE OF FUNDING NUMBERS PROGRAM ELEMENT NO.: N/A — PROJECT NO.: — TASK NO.: — WORK UNIT ACCESSION NO.:

11. TITLE (Include Security Classification)
Radio Frequency Hazard Monitoring - USAKA

12. PERSONAL AUTHOR(S)
Brown, David H.

13a. TYPE OF REPORT	13b. TIME COVERED	14. DATE OF REPORT (Year, Month, Day)	15. PAGE COUNT
Final	FROM 910221 TO 911021	TBD	TBD

16. SUPPLEMENTARY NOTATION
Prepared in Response to Small Business Innovative Research Topic A90-444.

17. COSATI CODES			18. SUBJECT TERMS (Continue on reverse if necessary and identify by block number)
FIELD	GROUP	SUB-GROUP	Radar, Radiation Safety, Safety/Survey, Mapping and Display

19. ABSTRACT (Continue on reverse if necessary and identify by block number)

This study provides the design of a network of sensors and procedures which will allow efficient and rapid mapping of RF power density and spectral data at a large number of ground station sensors surrounding the USAKA radars as a function of antenna pointing angles, transmitter power, and time of day. The system acts as a stand alone unit, powered by solar charged batteries. The sensor network is linked to a common control center, which collects, displays and archives the data. Communication between sensor units and the control center can use telephone or VHF radio links.

20. DISTRIBUTION/AVAILABILITY OF ABSTRACT	21. ABSTRACT SECURITY CLASSIFICATION
☐ UNCLASSIFIED/UNLIMITED ☐ SAME AS RPT. ☒ DTIC USERS	U
22a. NAME OF RESPONSIBLE INDIVIDUAL David H. Brown, P.E.	22b. TELEPHONE (Include Area Code) 918-299-2621 — 22c. OFFICE SYMBOL

DD Form 1473, JUN 86 — Previous editions are obsolete. — SECURITY CLASSIFICATION OF THIS PAGE

RADIO FREQUENCY HAZARD MONITORING - USAKA

FINAL REPORT

SBIR Topic A90-444

For the Period February 21, 1991 through October 21, 1991

Submitted to

U.S. ARMY STRATEGIC DEFENSE COMMAND
ATTN: CSSD-AT-E/John F. Phillips
P.O. Box 1500
Huntsville, AL 35807-3801

Contract No. DASG60-91-C-0027
CDRL A002

Effective Date: 21 February 1991
Expiration Date: 21 August 1991 extended to 21 October 1991

AEROMET/TUL 9110151

Submitted by

David H. Brown, Principal Investigator/Project Manager
918-299-2621 or DSN 956-5546

Aeromet, Inc.
P.O. Box 701767
Tulsa, OK 74170-1767

November 19, 1991

TABLE OF CONTENTS

LIST OF FIGURES

LIST OF TABLES

LIST OF ABBREVIATIONS

A/D	Analog to Digital
ALTAIR	ARPA (Advance Research Projects Agency) Long Range Tracking and Instrumentation Radar
ARRL	American Radio Relay League
CMOS	Complementary Metal-Oxide Semiconductor
COP	Computer Operating Properly
DDRR	Directional Discontinuity Ring Radiator
DSP	Digital Signal Processor
EEPROM	Electrically Erasible Programmable Read Only Memory
HCMOS	High-Density Complementary Metal-Oxide Semiconductor
HMOS	High-Density Metal-Oxide Semiconductor
IF	Intermediate Frequency
KREMS	Kiernan Reentry Measurement Site
RAM	Random Access Memory
RF	Radio Frequency
ROM	Read Only Memory
SCI	Serial Communication Interface
SPI	Serial Peripheral Interface
UHF	Ultra High Frequency
USAKA	United States Army Kwajalein Atoll
VHF	Very High Frequency
VME	Versa-Module Euro
WORM	Write Once Read Many

ACKNOWLEDGEMENTS

The assistance of laboratory technicians William "Dub" Sossamon and John Loftus was invaluable during the testing phase of the antenna element design.

Phillip K. Brewer, Senior Electrical Engineer, contributed to the microprocessor design.

The illustrations were drafted by Derek Thomas.

Testing at Roi-Namur was conducted by Ron Kuratsu, Engineer, Kwajalein Weather Station.

Composing and layout was done with the assistance of Beth Lanktree.

1. EXECUTIVE SUMMARY

Aeromet has proposed to develop a sensor system for the purpose of monitoring RF[1] field strength energy and sources. The sensor system is comprised of a control center and multiple sensor units. Phase I concentrated on the design and development of a unique programmable sensor that responds to RF energy in various frequency hazard bands. The sensor can be incorporated into a stand alone unit and be powered by solar charged batteries. The sensor unit is designed so that many of them can be operated in conjunction with a common control center which is used to change the mode of the sensor units and to collect, display, and archive the RF energy data. Communication between sensor units and the control center is via radio link. An extension to the contract was requested and granted so that RF testing could be completed at KREMS[2] in order to select a suitable frequency for the radio link. **Figure 1-1** shows how a typical installation might appear.

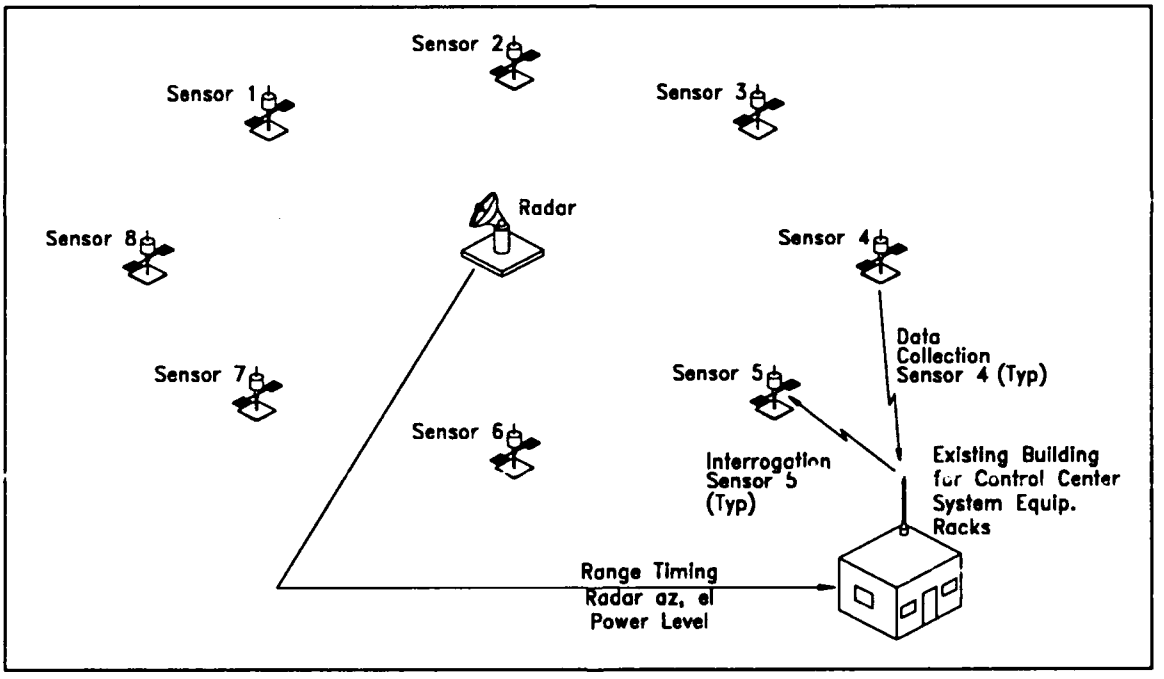

Figure 1-1 Typical Sensor System

Phase I work proceeded with scheduled research, investigation and test of sensor elements to determine which are feasible for sampling RF hazard energy. Concurrently, microprocessor technology was investigated for both the sensor unit and the control

---

[1] RF Radio Frequency

[2] KREMS Kiernan Reentry Measurement Site

center. Information gained from technical interchange with the Range, research, investigations, and testing was compiled in making this Phase I report. These efforts and results will be used as a data base for a Phase II proposal which will follow this submittal. Sensor research is covered in Chapters 2 through 4. System design is featured in chapters 6 through 9. Conclusions are summarized in Chapter 10.

Use of this sensor system is beneficial to both the operators of sites such as KREMS and those personnel who work at the sites. Personnel working near areas of intense radiation will be reassured knowing that the work areas are monitored and that hazard levels are not exceeded. They will be able to see that RF radiation dosage limits are not exceeded over time.

Operators of the site will have RF radiation dosimetry data necessary to combat lawsuits which may emerge from personnel illness which may be claimed due to exposure to RF radiation.

2. SENSOR FEASIBILITY RESEARCH

A literary search was conducted to determine the advantages and disadvantages of sensor types and configurations. The search concentrated on various antenna types feasible for application to RF hazard radiation detection and monitoring.

2.1 Feasibility Research

The goal of the feasibility research was to obtain an antenna with switchable or broadband elements which can be adapted and calibrated to receive energy in the RF hazard frequency spectrum required at USAKA[3], more specifically KREMS located on the island of Roi-Namur. Instruments are available which measure E field energy with one probe type and **H** field energy with another probe type. Most of these instruments combine the energy from all signal sources to an element or series of elements and measure the electric current times voltage or power produced in a manner similar to a standard power meter. More accurate power measurements are obtained when the energy is converted to heat as in a calorimeter.

If the energy is separated into various frequency bands, the offending radiation source can be easily identified and corrected. RF radiation is divided into two main groups, magnetic field radiation (**H** field) and electric field radiation (E field). E field radiation is commonly linked and dominant in the far field relative to the RF source while **H** field radiation is commonly linked and dominant in the near field relative to the RF source.

Table 2-1 shows the distance to the far field for the various KREMS radars. Because the radars to be monitored operate with parabolic reflectors, the following equation describes the distance to the far field.

$$\text{Far Field} = 2d^2/\lambda$$

Where d = diameter of reflector in meters
and λ = wavelength in meters

Since it is known for shorter distances (near field) that the **H** or magnetic field is a dominant factor in radiation (reference 1), a method must be provided for measurement of the **H** field. In most cases, the near field encompasses the entire island of Roi-Namur, as the greatest distance between any two points on Roi-Namur is 8,006 feet or 2,440 meters. See **Figure 2-1**. From **Table 2-1**, we can see that all of the radiation sources provide substantial near field radiation.

---

[3] USAKA United States Army Kwajalein Atoll

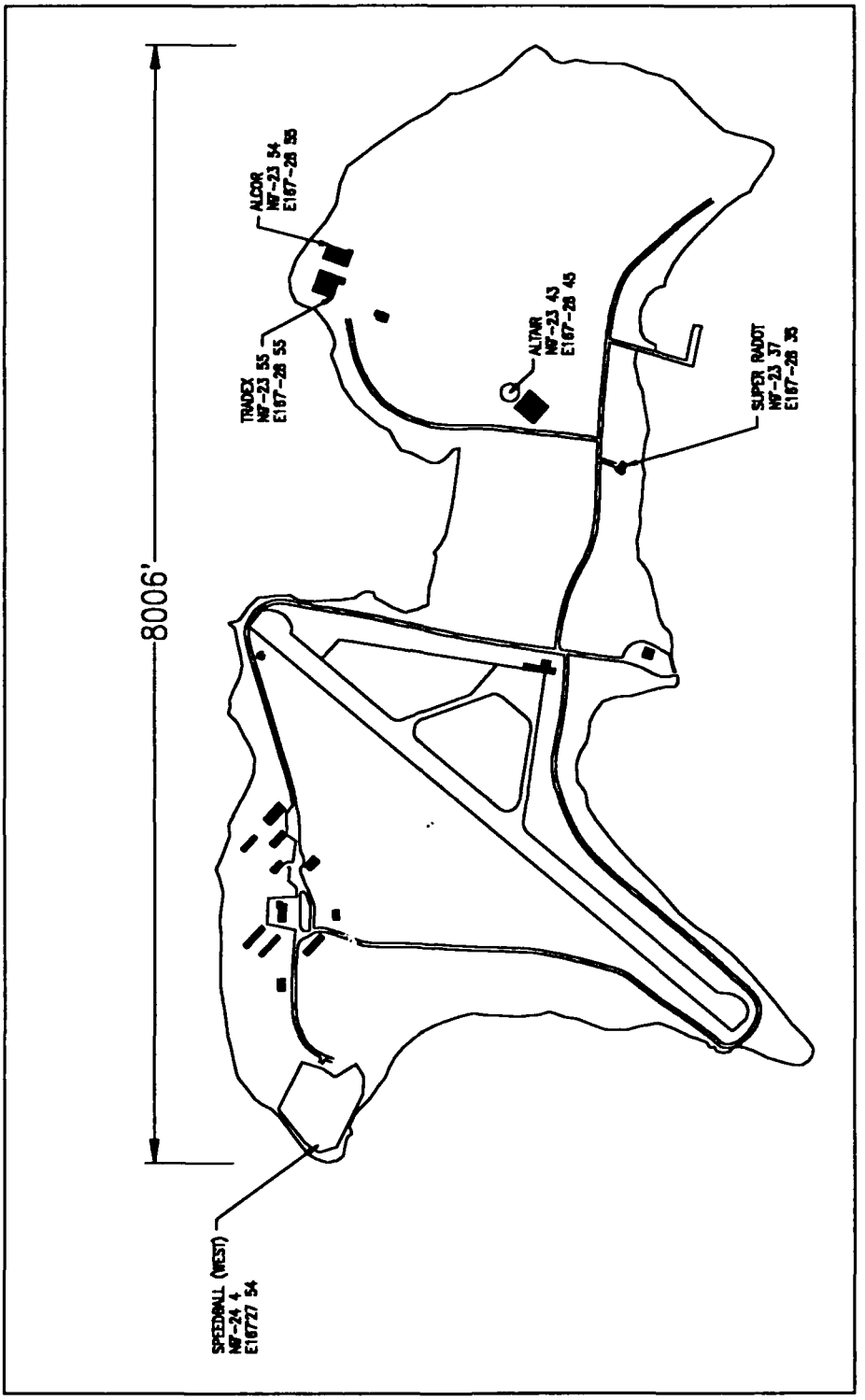

Figure 2-1 Island of Roi-Namur

Table 2-1 Distance to Far Field

Freq MHz	Radar	d Meters	Lamda Meters	Far Field Meters	Far Field Feet
162	ALTAIR	45.7	1.852	2,436	7,992
422	ALTAIR	45.7	0.711	5,874	19,272
1,320	TRADEX	25.6	0.227	5,774	18,945
2,950	TRADEX	25.6	0.102	12,889	42,289
5,672	ALCOR	12.2	0.053	5,627	18,462

The Aeromet probe concept involves the development of isotropic antenna elements which are precalibrated and can be switched via microprocessor control to sense radiation (both **E** and **H** field) in the various radar frequency hazard bands and provide this information to a common control center for further processing and storage.

Conventional probes, such as the Narda Broadband Isotropic Radiation Monitor, are designed to sense a wide range of RF energy incident on the probe at any angle. It is limited to measuring either **E** or **H** fields, one at a time, depending which probe type is connected to the instrument. The instrument response, through electronic means, fits the allowable radiation curve **(Figure 2-2)** shown in ANSI C95.1-1982. The radiation is then be read out in mW/cm^2 or a percent of maximum allowable radiation energy.

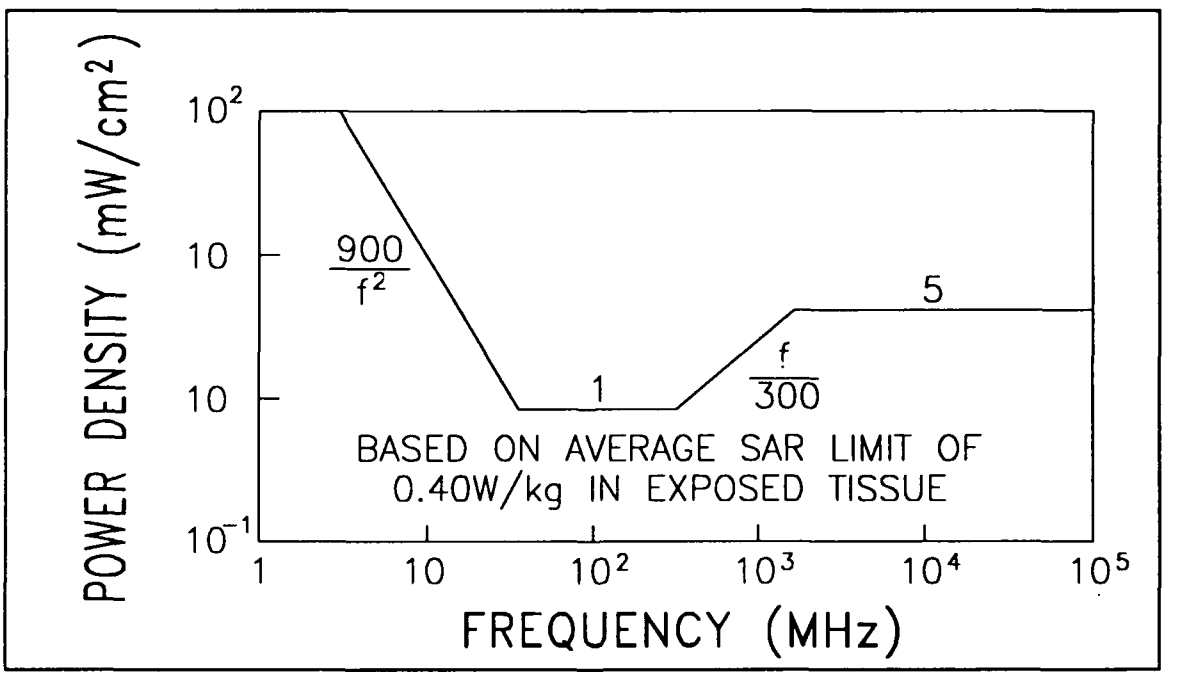

Figure 2-2 Radiation Power Level, Radio Frequency Protection Guide

The Aeromet probe concept senses the spectral distribution of RF hazard energy in both the **E** and **H** fields in the frequency bands required. Instead of providing a matched anticurve of **Figure 2-2**, the Aeromet probe is calibrated in those frequency bands required. The energy is then compared to the curve data, which is stored in the microprocessor memory, and the radiation level (or percent of maximum) is thus obtained.

Because potential spectral bands of radiation are known, probe design is simplified. Probe element lengths were designed in frequency band multiples which eliminates major peaks and valleys in the response of the elements. Use of this concept simplifies a perplexing set of variables for probe element design.

Numerous sources were reviewed in a search to find suitable antenna elements that are non-polar, small in size, easily mass produced, inexpensive, insensitive to orientation, broadbanded, and/or remotely switchable for multi-band operation.

Many sources were investigated during the antenna element research (references 1, 2, 3, 4), since microstrip technology seemed appropriate for this application. Use of active endfire antennas using notch techniques were investigated. Frequency agile microstrip antennas were investigated for use in the frequency bands from L-band through C-band. Turnstile and crossed dipole antennas were investigated for use in VHF[4], UHF[5] and L-bands. Use of active integrated antenna elements was also considered. The ARRL[6] Handbook (reference 5) was found to be useful for reviewing techniques for fabricating practical antenna element types.

Several of the following antenna types appeared to be feasible for E field detection at first blush. They include the dipole, vertical dipole, turnstile, leaky wave, DDRR[7], notch, microstrip, and active integrated element antennas.

Selection of the antenna element type was straightforward because there are only a few types that can fulfil the diverse needs required. Many antenna types are highly directional and offer gain. However, gain is not a consideration since the field strengths to be measured are relatively high. Ultimately, a variation of the turnstile antenna (a tri-axial crossed dipole, see **Figure 2-3**) was chosen for the E field sensing element, although the microstrip antenna seemed a likely candidate for the higher frequency bands.

---

[4] VHF Very High Frequency

[5] UHF Ultra High Frequency

[6] ARRL American Radio Relay League

[7] DDRR Directional Discontinuity Ring Radiator

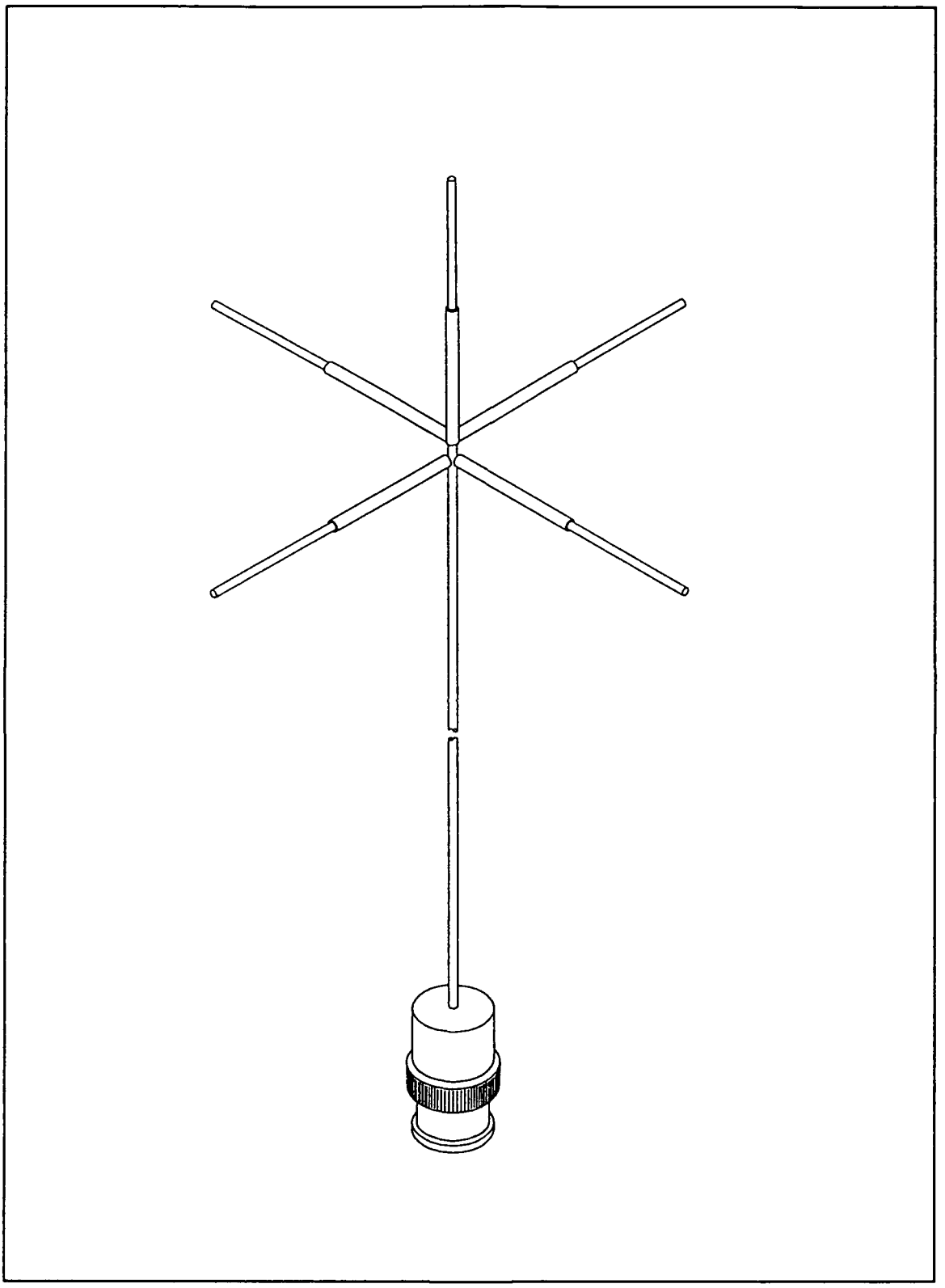

Figure 2-3 Tri-Axial Crossed Dipole E Field Sensor

A tri-axial coil arrangement is required for H field sensing. **Figure 2-4** shows a design that was tested.

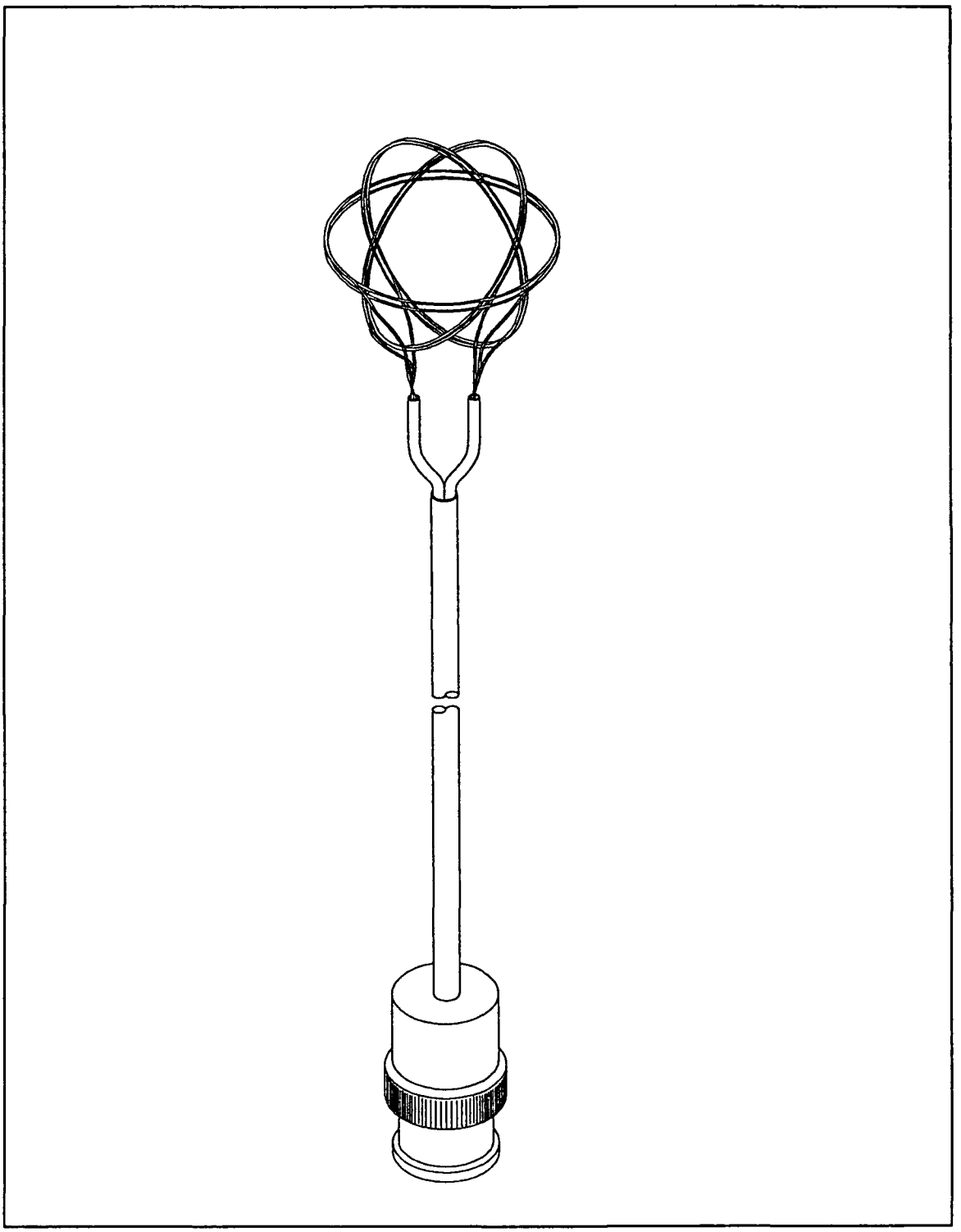

Figure 2-4 Tri-Axial Coil Arrangement H Field Sensor

Of the 8 antenna types previously listed, only three were seriously considered for use as the E field sensor element. The others were eliminated due to failing one or more of the operational criteria. Antenna types that appeared more feasible than the others include the tri-axis dipole, the microstrip, and the DDRR.

A tri-axis dipole can be constructed so that its resonance is between hazard bands. In this way peaking is avoided and it can be calibrated rather easily for the intended frequencies of use. The elements can be set up in series, or outputs can be added in a combiner. **Figure 2-5** shows a tri-axis dipole element E field sensor assembly which can be used with a combiner.

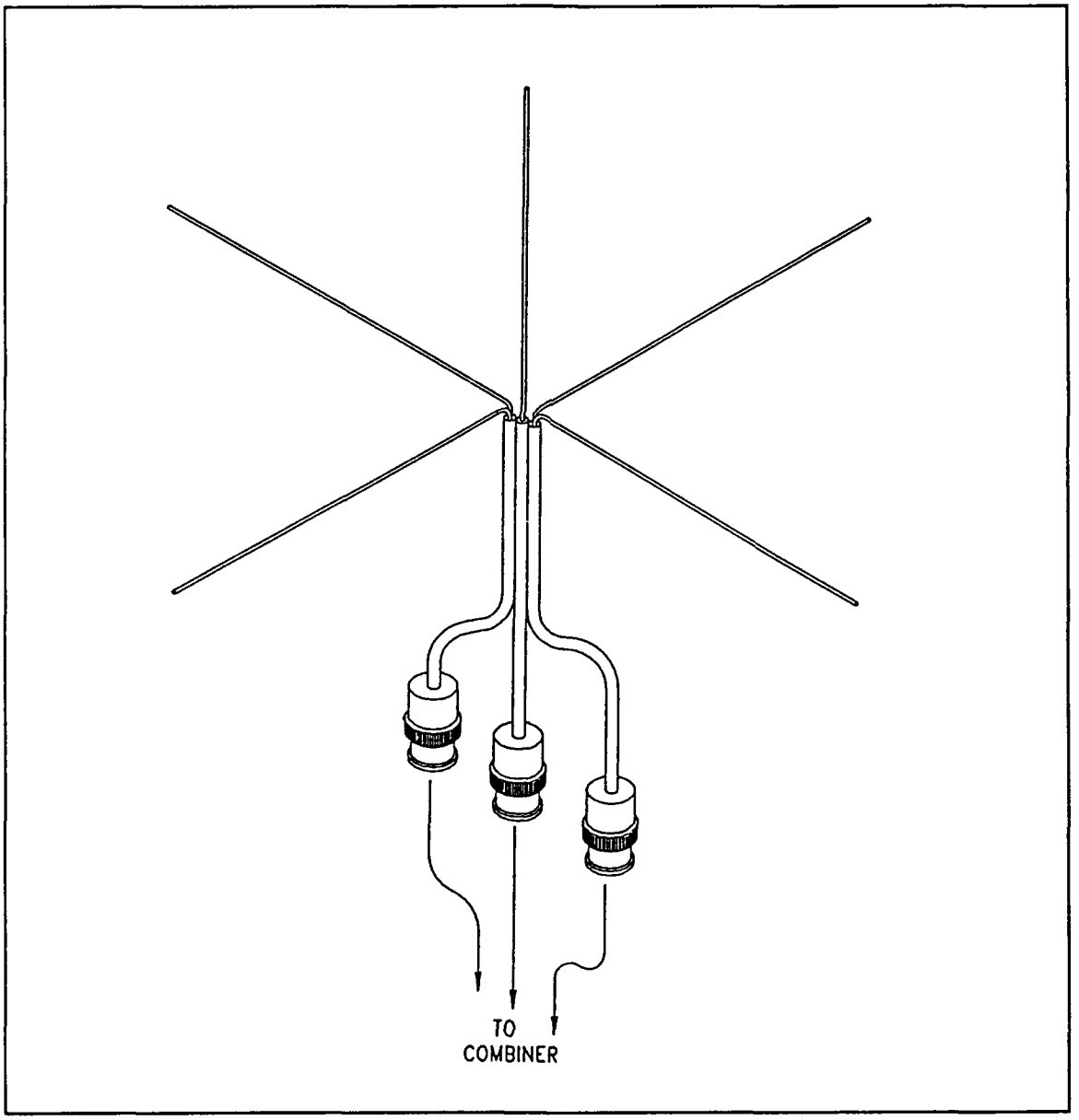

Figure 2-5 Tri-Axis E Field Sensor for Use With a Combiner

Microstrip antennas have inherently low bandwidths (in the order of 2%) so they were not initially considered viable for this application. However, research (reference 6) has shown that there are ways to broaden the bandwidth to an acceptable level. Research of microstrip antennas shows how to extend bandwidth as much as 30%. See **Figure 2-6.**

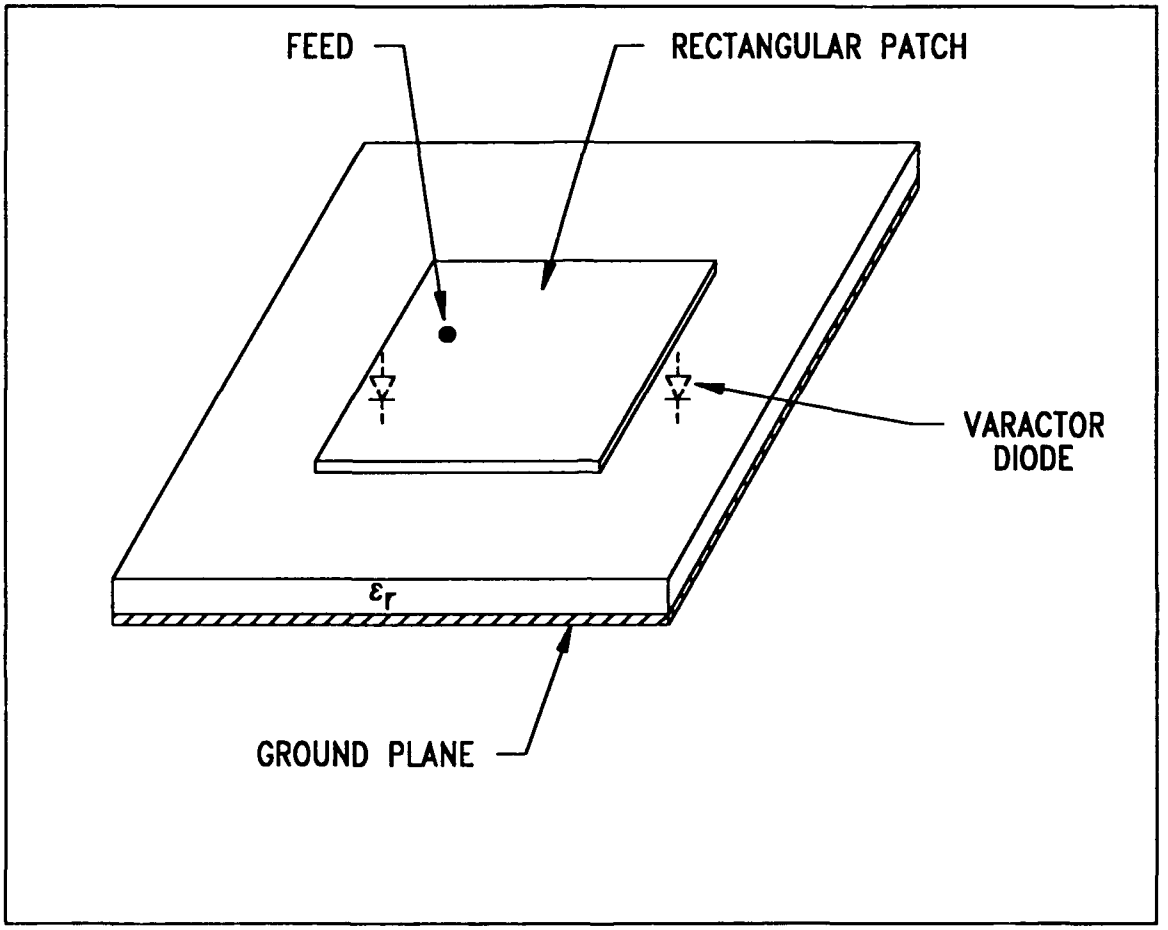

Figure 2-6 Patch Style Micro Strip Antenna Element Sensor

The DDRR antenna, see **Figure 2-7**, seems practical at lower frequencies, but tuning values make it impractical for use at higher frequencies. Also, bandwidth is somewhat limited for this antenna (reference 5). Additionally, it does not discriminate well between **E** and **H** fields.

Only the dipole and the microstrip elements were serious candidates for the **E** field sensor, although all three types were evaluated.

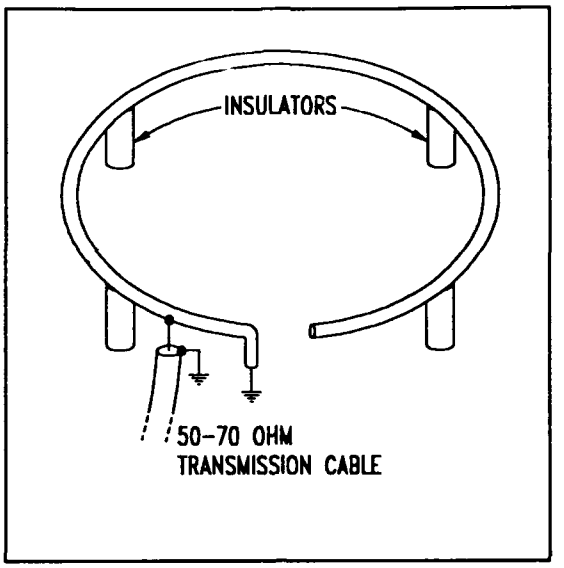

Figure 2-7 Directional Discontinuity Ring Radiator Sensor

2.1.1 Crossed Dipole Antenna

There are several variations to the crossed dipole antenna such as the turnstile (**Figure 2-8**), right or left circularly polarized, or tri-axial. It was hoped that one could be chosen that would ultimately lend itself to a printed circuit layout. Unfortunately, this was not possible. However, the tri-axial dipole antenna configuration appears most promising. See **Figure 2-3**.

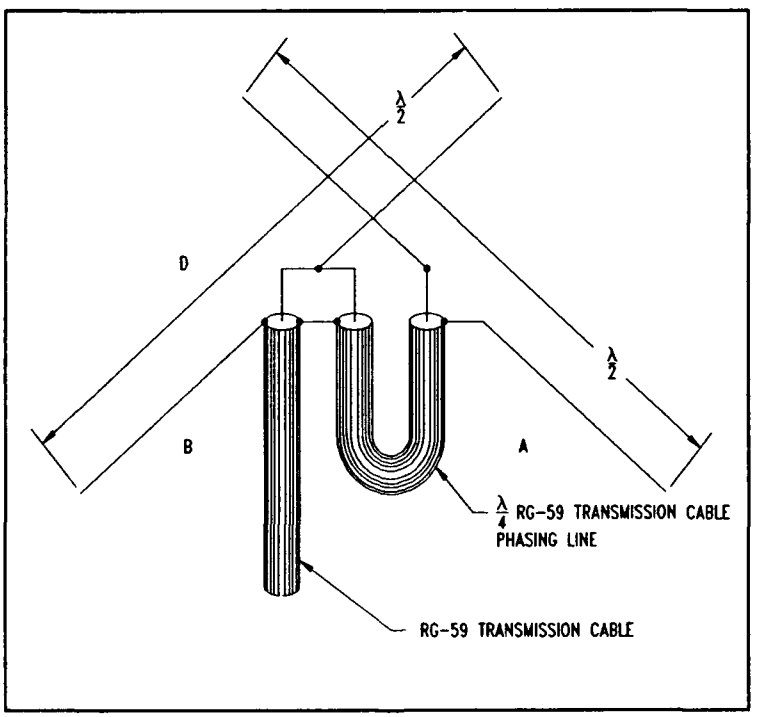

Figure 2-8 Typical Turnstile Sensor

2.1.2 Microstrip Antenna

The microstrip is a type of antenna which can exist in many configurations. See **Figure 2-9**. Its bandwidth can be extended by use of electronic varactor tuning or by use of 1/4 wave stub elements or by addition of parasitic elements. The shape of any of the elements is limited only by the designer's imagination. I favored use of circular patch elements because published test information is available for these elements. An advantage to this antenna type is that it can be constructed using printed circuit board technology.

2.1.3 DDRR Antenna

The DDRR antenna (see **Figure 2-7**) has known limitations; however, a basic VHF unit was constructed for testing purposes. Investigations were conducted to see what the difference in gain would be for signals "edge on" versus "head on". Many antennas, similar to this are designed to be used with a ground plane. Without the ground plane, impedance varies and the shape of the pattern becomes irregular.

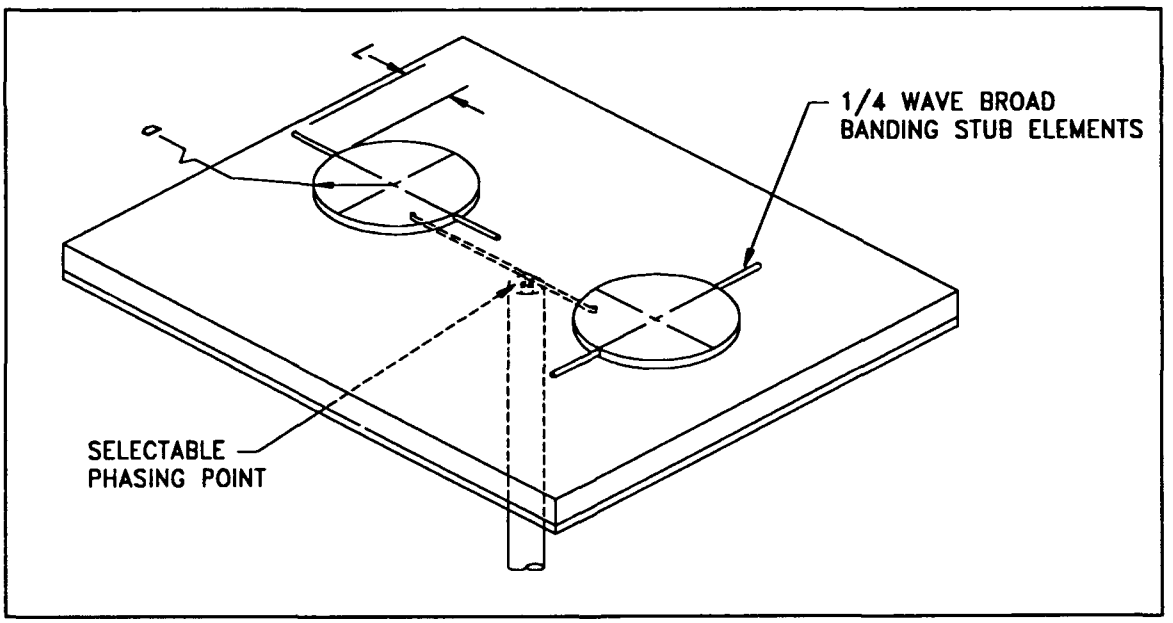

Figure 2-9 Microstrip Sensor Utilizing 1/4 Wave Broadbanding Stubs

3. SENSOR FEASIBILITY TESTING

3.1 Sensor Testing

The antenna elements were tested at a field test site located in Tulsa. Although no attempt was made to actually calibrate the elements, relative measurements were recorded to assure that they possessed good signal leveling qualities from band to band. Far field testing was conducted with the **E** field sensing elements and near field testing was conducted with the **H** field sensing coil assemblies.

Dipole test antennas were made for each of the frequency bands to be evaluated. **Figure 3-1** shows the general test setup for far field tests. Near field tests were conducted in the same manner, but in the near field. Near field testing was accomplished by use of a long coil for use as a transmitting antenna as shown in **Figure 3-2**. The **H** field was measured and found to be nearly uniform in the center of the cylinder throughout its useful length.

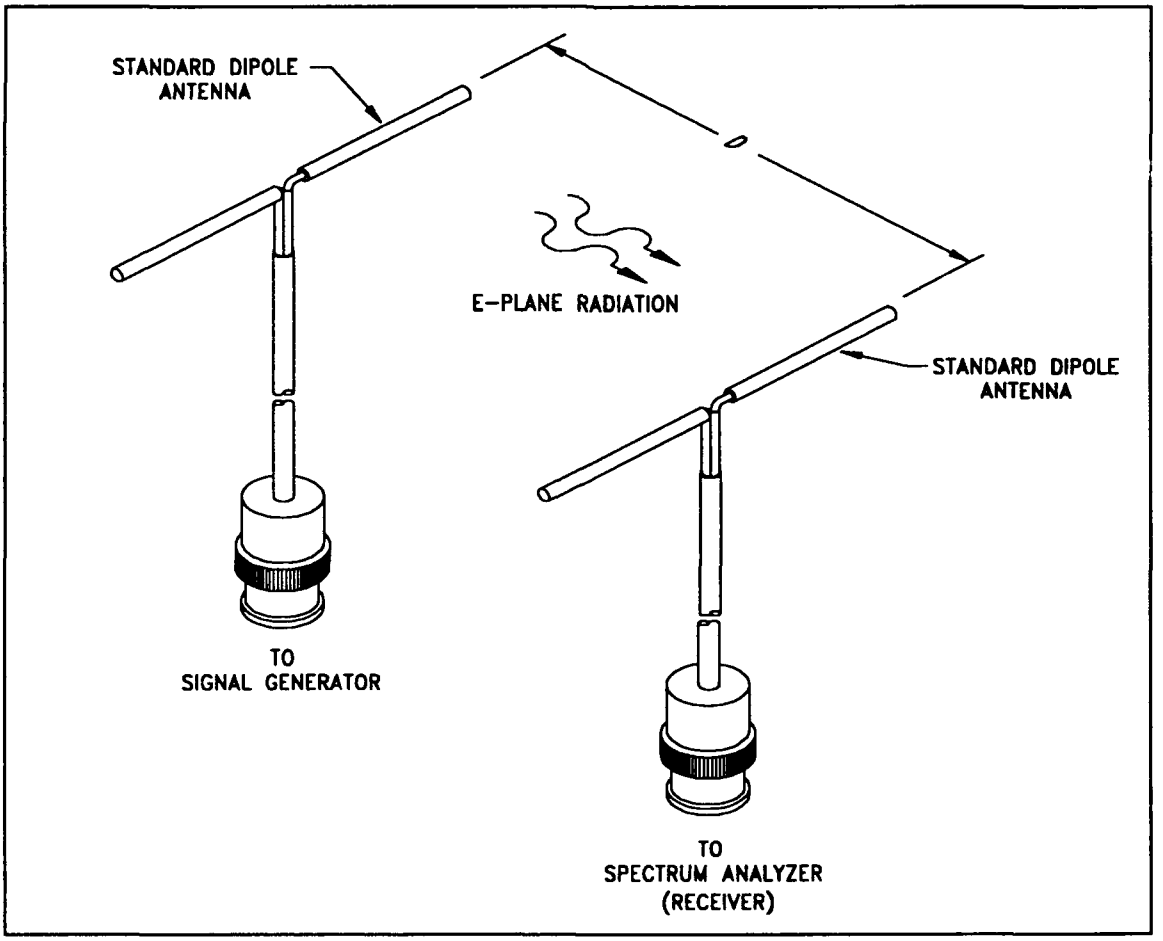

Figure 3-1 E Field Test Setup

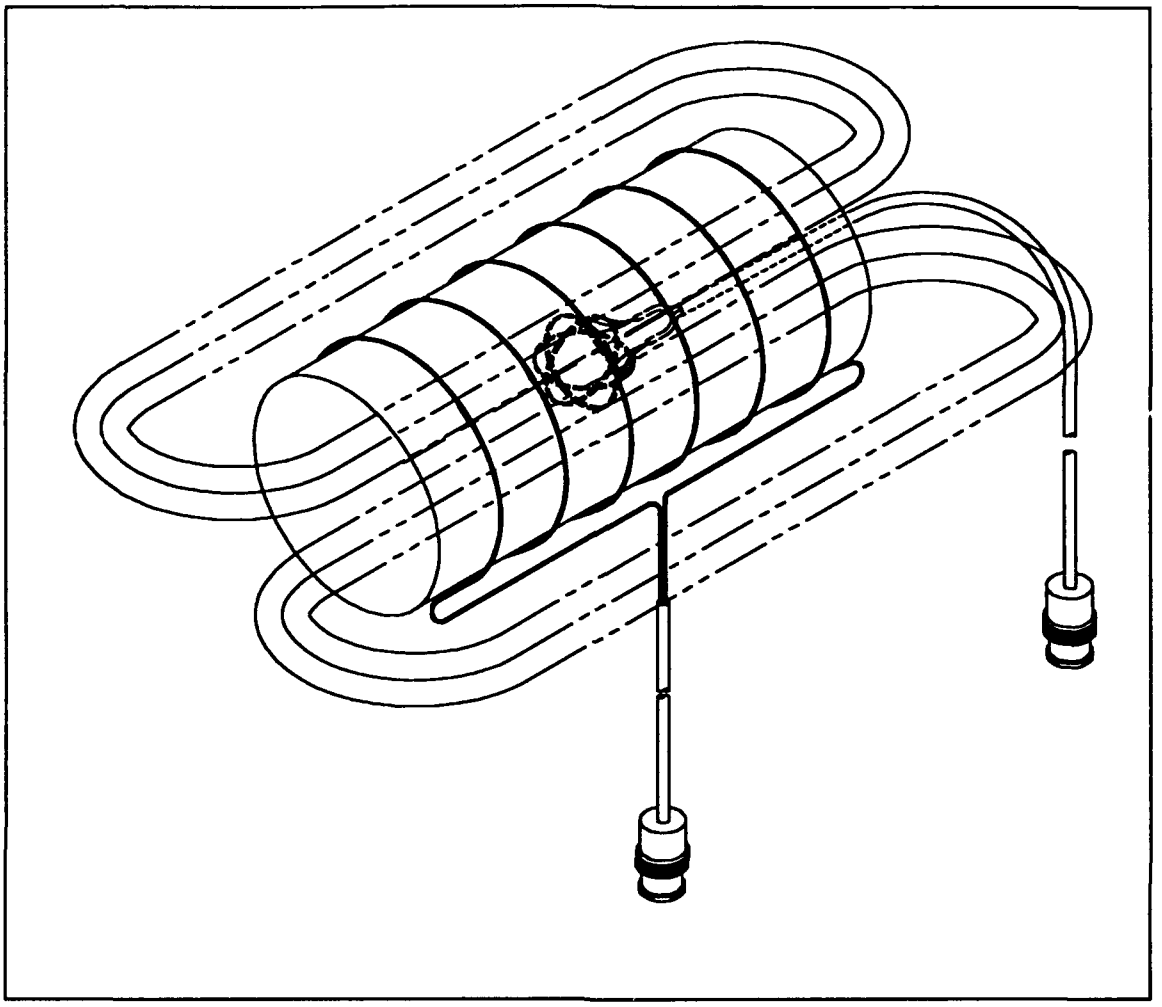

Figure 3-2 H Field Test Setup

3.1.1 Tri-Axis Element Testing

The two antenna substitution method was used to evaluate the tri-axis crossed dipole **E** field receiving element antenna and an equivalent **H** field antenna. The antennas were evaluated in the following bands:

1. VHF-band, 162 MHz; simulates ALTAIR
2. UHF-band, 422 MHz; simulates ALTAIR
3. L-band, 1,320; simulates TRADEX
4. S-band, 2,950 MHz; simulates TRADEX
5. C-band, 5,672 MHz; simulates ALCOR

The test procedure includes rotating the antenna about the support staff 360 degrees and rotating the antenna through 90 degrees as shown in **Figure 3-3**.

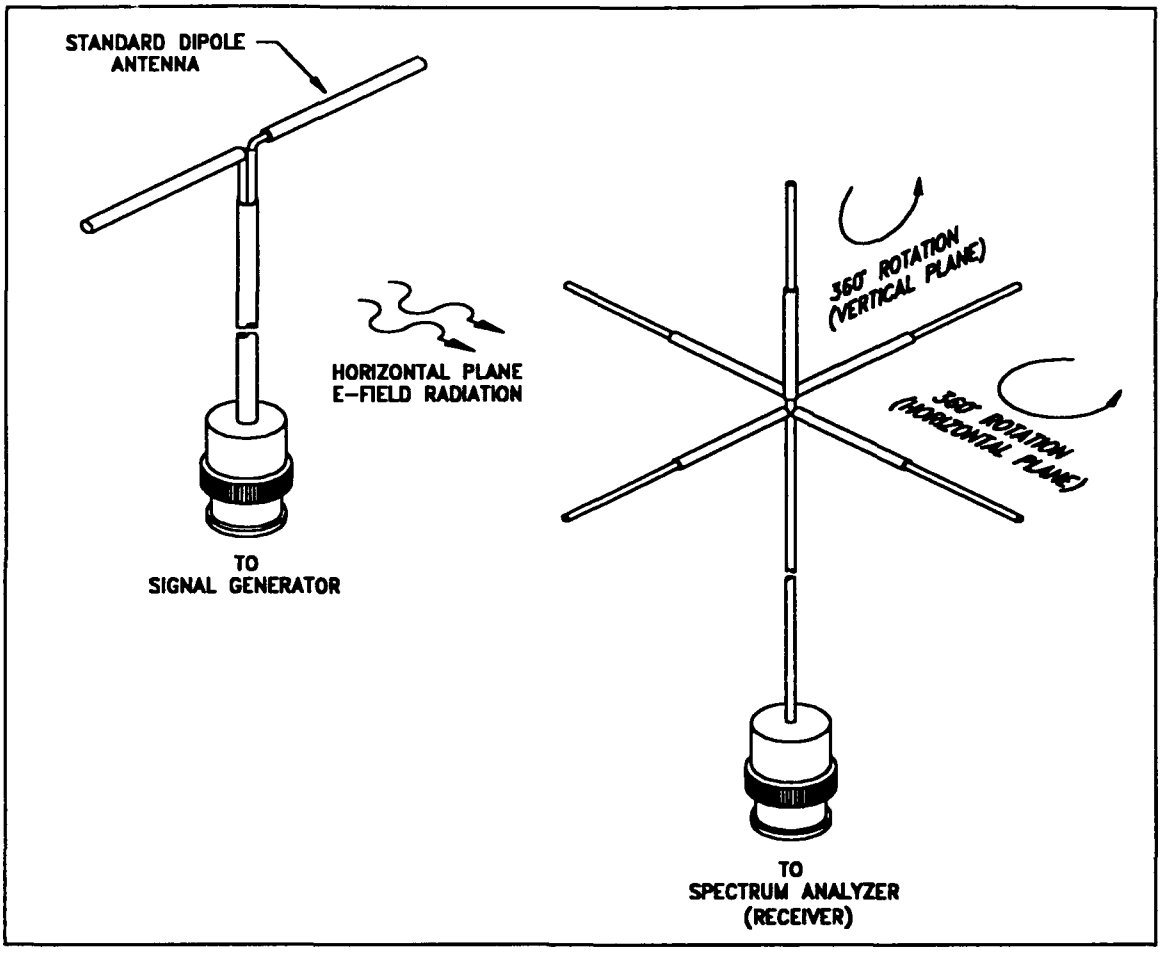

Figure 3-3 E Field Testing Method

3.1.1.1 Band 1, VHF 162 MHz

Test set antennas were fabricated for this band and are shown in **Figure 3-4**. The tri-axis dipole antenna for this band was fabricated as shown in **Figure 2-3**.

Chart 3.1 contains the test data for tests of the **E** field antenna and Chart 3.2 contains the test data for tests of the equivalent **H** field antenna. See **Appendix I.**

3.1.1.2 Band 2, UHF 422 MHz

Test set antennas were fabricated for this band and are shown in **Figure 3-4**. The same **E** and **H** field antennas were tested at UHF.

Chart 3.3 contains the test data for tests of the **E** field antenna and Chart 3.4 contains the test data for tests of the **H** field antenna. See **Appendix I.**

3.1.1.3 Band 3, L 1,320 MHz

Test set antennas were fabricated for this band and are shown in **Figure 3-4**. The same **E** and **H** field antennas were tested at L-band.

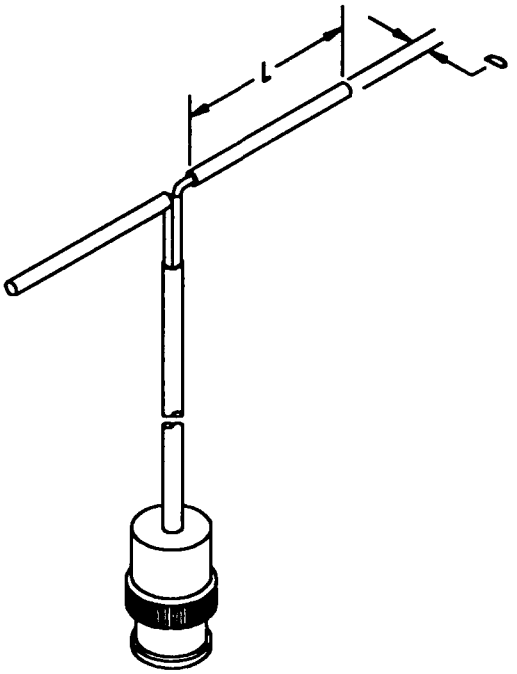

Frequency	L (inches)	D (inches)
162 MHz	17.68	0.690
422 MHz	2.17	0.270
1320 MHz	0.97	0.040
2950 MHz	0.97	0.020
5672 MHz	0.50	0.010

Figure 3-4 Standard Dipole Dimension Chart

Chart 3.5 contains the test data for tests of the **E** field antenna and Chart 3.6 contains the test data for tests of the **H** field antenna. See **Appendix I**.

3.1.1.4 Band 4, S 2,950 MHz

It was thought that the microstrip antenna would be a good candidate for both S- and C-bands. Test set antennas were fabricated for this band and are shown in **Figure 3-4**. The microstrip antenna was fabricated according to literature provided by P. Bhartia and I.J. Bahl and is shown in **Figure 2-9**.

Chart 3.7 contains the test data for tests of the S-band microstrip antenna. Results of the test were somewhat disappointing as the "edge on" response was not as good as anticipated. See **Appendix II.**

However, since we had such good results using the tri-axis E and **H** field antennas at other frequencies, it was decided to see what would happen if we used them at S-band. The results were extremely good and can be seen in Charts 3.8 and 3.9. See **Appendix I.**

3.1.1.5 Band 5, C 5,672 MHz

Test antennas were fabricated for this band and are shown in **Figure 3-4**. A microstrip antenna was also fabricated for this band. See **Figure 2-9**. Chart 3.10 contains the test data for tests of the C-band microstrip **E** field antenna. Test results were as disappointing as those obtained for the S-band tests. See **Appendix II.**

The encouraging results of the S-band tests using the standard tri-axis antennas prompted testing of them at C-band. Unfortunately, the signal generator malfunctioned and had to be sent for repair. Charts 3.11 and 3.12 are included for completeness. See **Appendix I.**

3.2 Sensor Test Conclusions

From the data gathered in the above tests, it appears that all bands up to X can be accommodated by use of the standard tri-axis sensors. One reason they are so adaptable is that they are used in the receive mode only and proper matching is not essential. The receiver has a fairly constant input impedance throughout the frequency range so that loading is relatively constant with frequency. The elements are operated below resonance, in most cases, so that peaking is not a problem. At the higher frequencies, the sensors become more efficient because they are closer to ideal design. The net result is reception of a fairly uniform signal level over the frequency range required.

4. SENSOR DESIGN

Since a relatively uniform signal is received across the frequency spectrum using the tri-axis antenna concept, it seems reasonable that it can be used without switching elements during hazard band changes.

The design of the antenna elements has been greatly simplified and frequency selection and identification is by detection of an IF[8] signal which is produced by microprocessor selection of an appropriate local oscillator frequency. If preselection filters are required, they can be electronically inserted by the microprocessor.

Design of the E field sensor is shown in **Figure 2-3**. A more detailed drawing is shown in **Section 6**. Because the design is based on a classic dipole, the design is straightforward and the dipoles were added in parallel. On the other hand, coil sensors or **H** field antennas are not usually addressed in classical antenna handbooks. Therefore, a detailed presentation of the **H** field sensor development follows. Design of the tri-axis **H** field sensor is shown in **Figure 2-4**.

An antenna was fabricated that serves the function of generating an **H** field. It consists of a coil 3 inches in diameter and 6 inches long. It is wound with 5 turns of # 18 enamel coated wire. See **Figure 3-2**.

$L = r^2n^2/(9r + 10l) = (1.5)^2(5)^2/[9(1.5) + 10(6)] = 0.76\ \mu h$

$B = (E)10^8/4.44NAF,$

where E = volts, RMS

N = number of turns = 5

A = area in cm^2 = $45.6cm^2$

F = frequency = 162 MHz

B = **H** field in gauss = 766 μgauss

Power applied was 15 dBm.

$P = 10 \log P_2/P_1$

$15\ dBm = 10 \log P_2/0.001$

$P = E^2/R$

Let R = 50 0hms

$E = [(0.03162)(50)]^{1/2} = 1.257$ volts, RMS

---

[8] IF Intermediate Frequency

The receiver coil was fabricated from 2 turns of #22 enamel coated wire wound on a 1 inch diameter mandril.

$L = r^2n^2/(9r + 10l) = (0.5)^2(2)^2/[(9)(0.5) + (10)(0.1)] = 0.1818\ \mu h$

$E = 4.44NAfB$

where $A = 5.067\ cm^2$

$N = 2T$, where T is number of turns

$f = 162$ MHz

$B = 766\mu$ Gauss

$E = 0.0558$ VRMS

Now, received power should be $E^2/R = 62\ \mu$ watts and

$dBm = 10 \log (0.062/1) = -12.07$

A tri-axis coil was fabricated from this data and the coil outputs were added in series. The tri-axis coil assembly was used in conjunction with the transmitting coil described above. The tri-axis coil was able to sense the transmitted B field at between -12 and -12.2 dB for any orientation of the tri-axis receiving coil. As can be seen, the test data agrees nicely with the calculated design. A data sheet for this test is included as **Appendix IV**, Chart 13.

5. ASSESSMENT OF RANGE REQUIREMENTS

Contact with USAKA was made early in the program through Project Technical Monitor, John Phillips, to assure that Phase I work is serving the needs of the end user. Advice was sought pertaining to the radars that should be monitored and possible frequencies to be used for communications/telemetry links between sensor units and the control center.

Dave Villeneuve, USAKA Range Safety, was assigned to the project. Also, contacted was Michael Austin at MIT Lincoln Lab. He suggested that the sensing elements be covered with a radome so that salt buildup can be easily washed (cleaned) on a regularly scheduled basis. He also suggested that I contact Dr. Michael Burrows for information pertaining to ALTAIR[9].

Dr. Burrows was very helpful and suggested that a test be conducted to see if the proposed VHF communication frequency at 200 MHz affects the ALTAIR receiving sensitivity or circuitry. He also suggested that we contact Gary Cleveland at the Safety Office on Roi-Namur.

Gary Cleveland was most interested in our research and related that "the island is currently conducting the most detailed radiation tests that have been attempted in many years." Sixteen Narda radiation monitors were purchased for a series of tests which are scheduled to take at least a year to complete. Both E field and H field probes are being used in the tests. As can be seen, a year is a long time to work on one survey. The Aeromet sensor plan could complete the same survey in a fraction of the time and provide constant dosimetry data as well.

---

[9] ALTAIR ARPA (Advance Research Projects Agency) Long Range Tracking and Instrumentation Radar

6. PRELIMINARY DESIGN OF A STAND ALONE SENSOR UNIT

The sensor unit is designed so that it can operate for weeks without maintenance or physical contact by operators. To be able to do this, several basic design features were considered.

1. Communication between the sensor unit and the control center must be by telemetry.
2. The power source must be large enough to withstand several weeks of uninterrupted operation. Solar charged batteries meet this goal.
3. The unit should have a self check function and report malfunctions so that bad data will not contaminate the data base. The microprocessor and associated circuitry provide this function.
4. The unit should have a way of keeping track of time. The microprocessor also provides this function.
5. The unit should be able to change its function on command from the control center to accommodate the needs of the Range. The communications/telemetry system together with the microprocessor provides this function.

6.1 Sensor Unit Configuration

A cylindrical container is a practical and space efficient design for housing the sensor, electronic control circuitry, and data acquisition circuits. All of the antenna elements can be located on the circular top end of the cylinder. The multiband-3-axis-crossed dipole antenna for **E** field detection can be located on the top surface together with the 3-axis coil assembly for **H** field detection. A plastic or fiberglass radome will cover the sensor antenna elements and serve as both a static shield and a weather shield. The radome may require periodic washing to remove salt spray deposits which could affect the sensitivity of the unit. Various band phasing elements can be located below the antenna mounting surface, if required, along with the electronic circuitry. A vertical antenna, to be used as part of the communications network between the sensor units and the control center, can be installed on the bottom of the cylindrical sensor unit as an integral part of the support stand. This is possible because the support pole is to be fabricated with plastic pipe. **Figure 6-1** shows a preliminary layout of the sensor unit's RF detection components, radome, and communications or telemetry antenna.

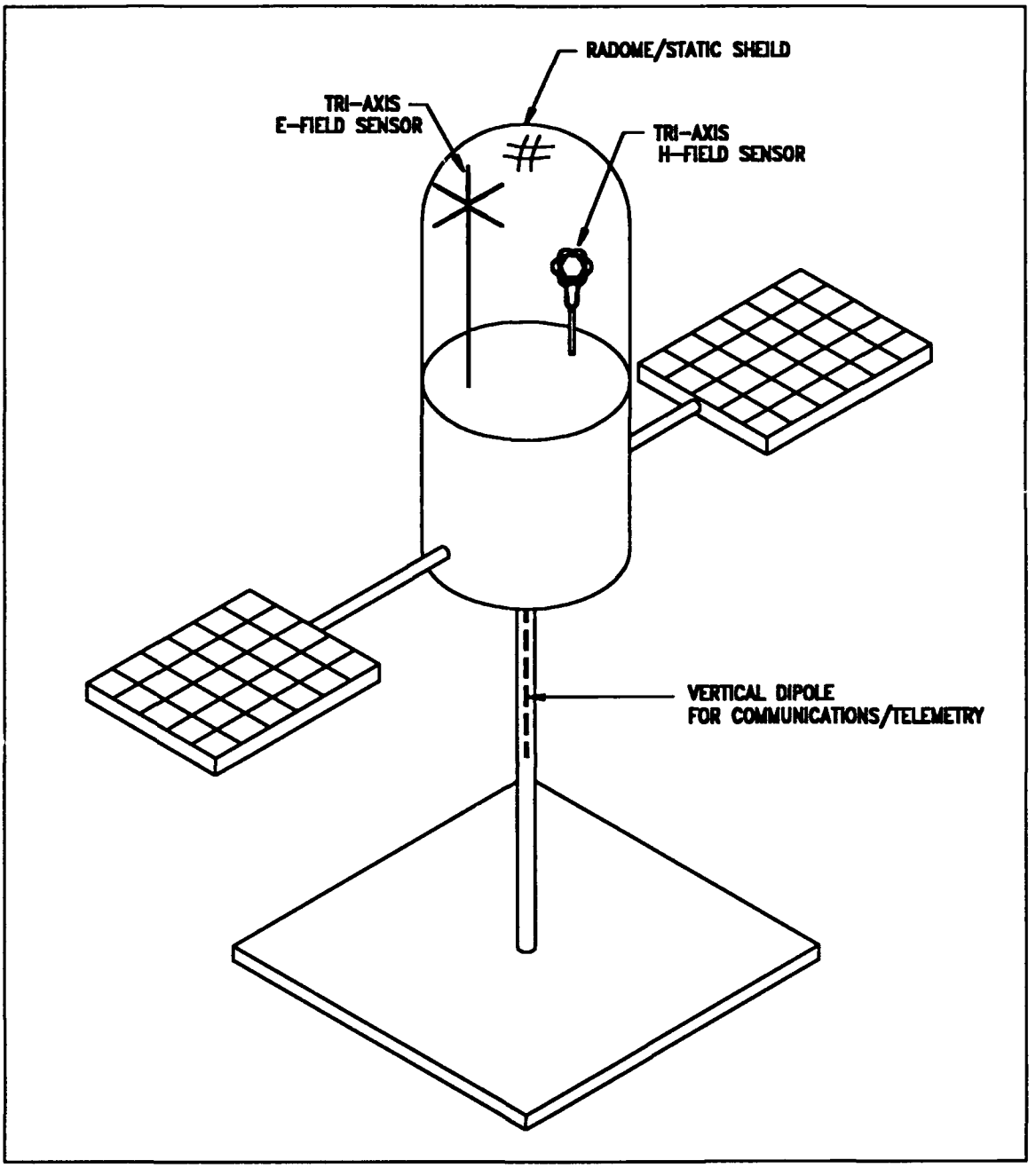

Figure 6-1 Sensor Unit

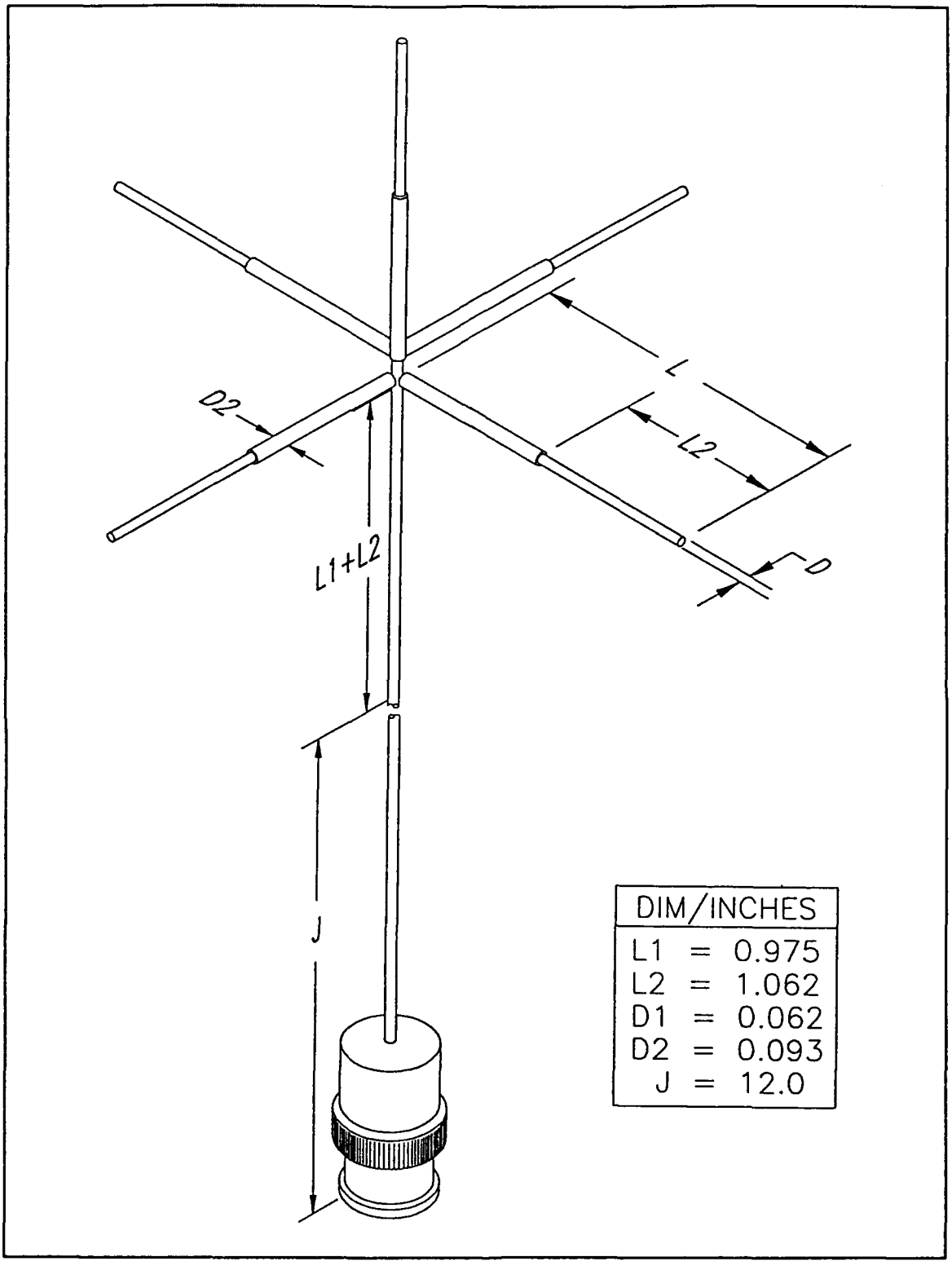

Figure 6-2 E Field Sensor Design

6.2 Antenna Elements

The intensive investigation and testing of sensor elements has allowed suitable antenna element designs to be developed during this Phase I effort. Since the design was tested, little risk will be encountered for Phase II efforts. Refer to **Figure 6-2** for the **E** field design and **Figure 6-3** for the **H** field design.

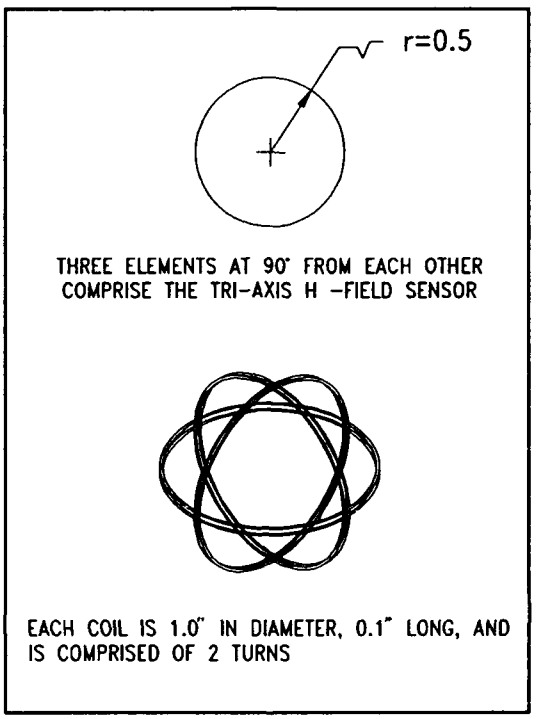

Figure 6-3 H Field Sensor Design

6.3 Receiver Front End

Figure 6-4 shows a block diagram of a receiver front end design that can be used in the sensor unit. In addition to the components shown, an electrostatic shield will be used to desensitize the detection system and prevent arcing in intense RF radiation fields. As can be seen, the only critical component is the wide band mixer that is required. A ring diode type using hot carrier diodes has been selected as the best candidate for the system. A microprocessor controlled attenuator will be used between the sensing elements and the mixer to prevent overloads. An additional benefit of the attenuator is that it will provide a relatively constant impedance for the sensor elements which will improve their linearity. An IF module will be selected to meet the needs of the system and is not a critical component because gain is low and bandwidth is relatively narrow. The main function of the IF module is to serve as a band to band filter/buffer.

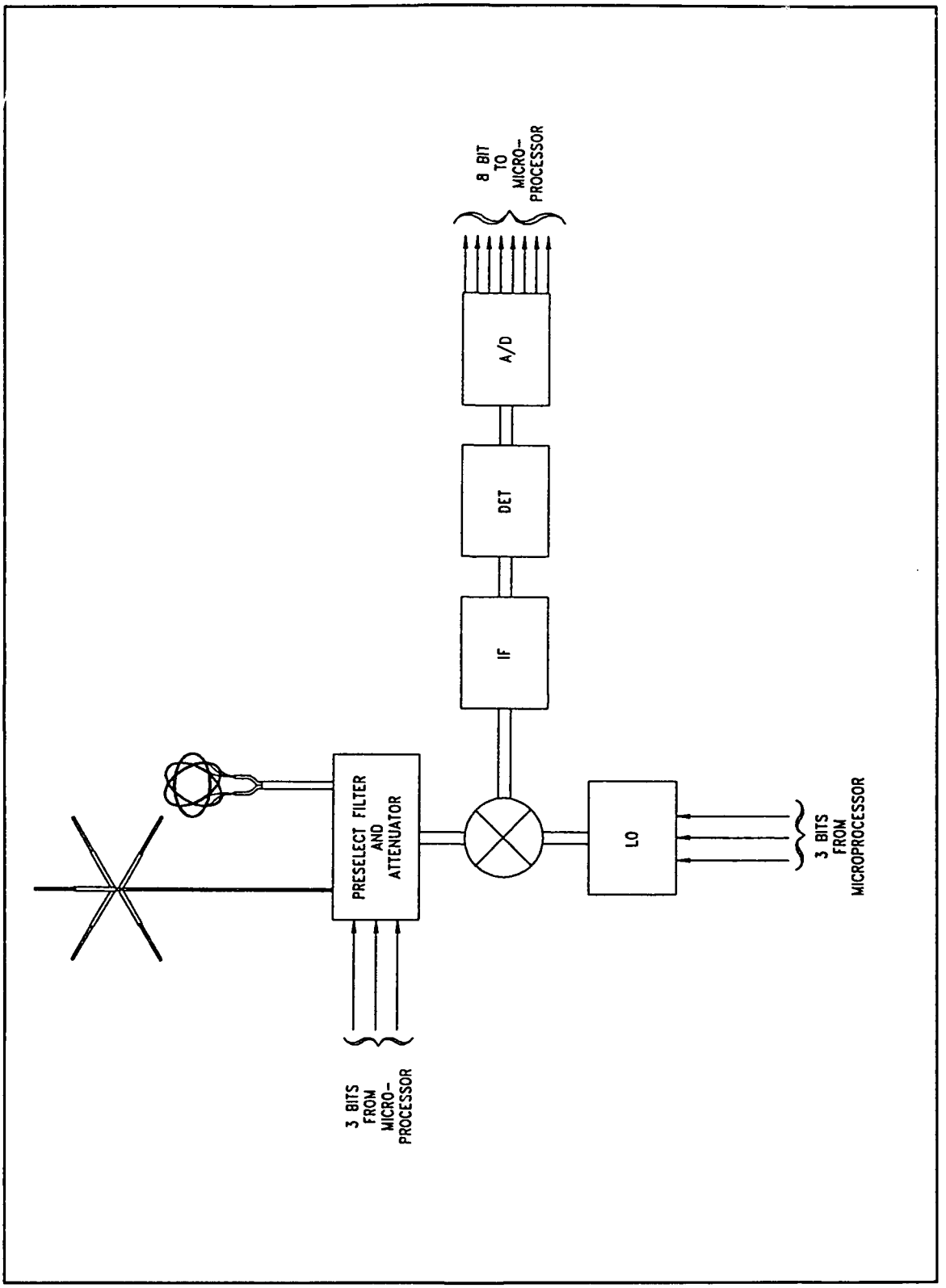

Figure 6-4 Sensor Receiver Front End

The local oscillator is a precision item and its output frequency will be controlled by the microprocessor. In theory, the oscillator will be stepped in frequency so that the IF will receive energy from each of the required hazard bands on a time shared basis. Practically, the oscillator will hesitate at each frequency so that both **E** and **H** field antenna elements can be used to extract RF energy from exposure to the respective energy fields. There are two ways for this to occur. One is to have two separate front ends, one for the **E** field antenna and one for the **H** field antenna. Another way is to use the same front end for both measurements by time sharing the front end. This is the more cost effective way since the microprocessor can multiplex all readings for all bands in less than a fraction of a second.

The detector will provide a fast integration constant for the received RF hazard signals and pass this information to the A/D converter as a DC level associated with signal strength. This DC data will then be transferred to the microprocessor. The receiver will be blanked when the sensor unit is telemetering information to the control center.

6.4 Microprocessor

The Motorola MC68HC11A8 was chosen as the microprocessor to be implemented in the design for the sensor unit. A schematic/block diagram of the microprocessor is shown in **Figure 6-5**. As can be seen in the diagram, this microprocessor unit contains all the I/O that is required for this application. Additionally, the HC11 can operate at clock speeds from DC to 8 MHz. Current drain for the HC11 is relatively low during normal operation and it can be placed in a "WAIT/STOP" mode which draws even less current. This allows operation with the solar powered battery concept which is the basis for the unit's power supply design. Selection of the microprocessor is covered in detail in Section 7.

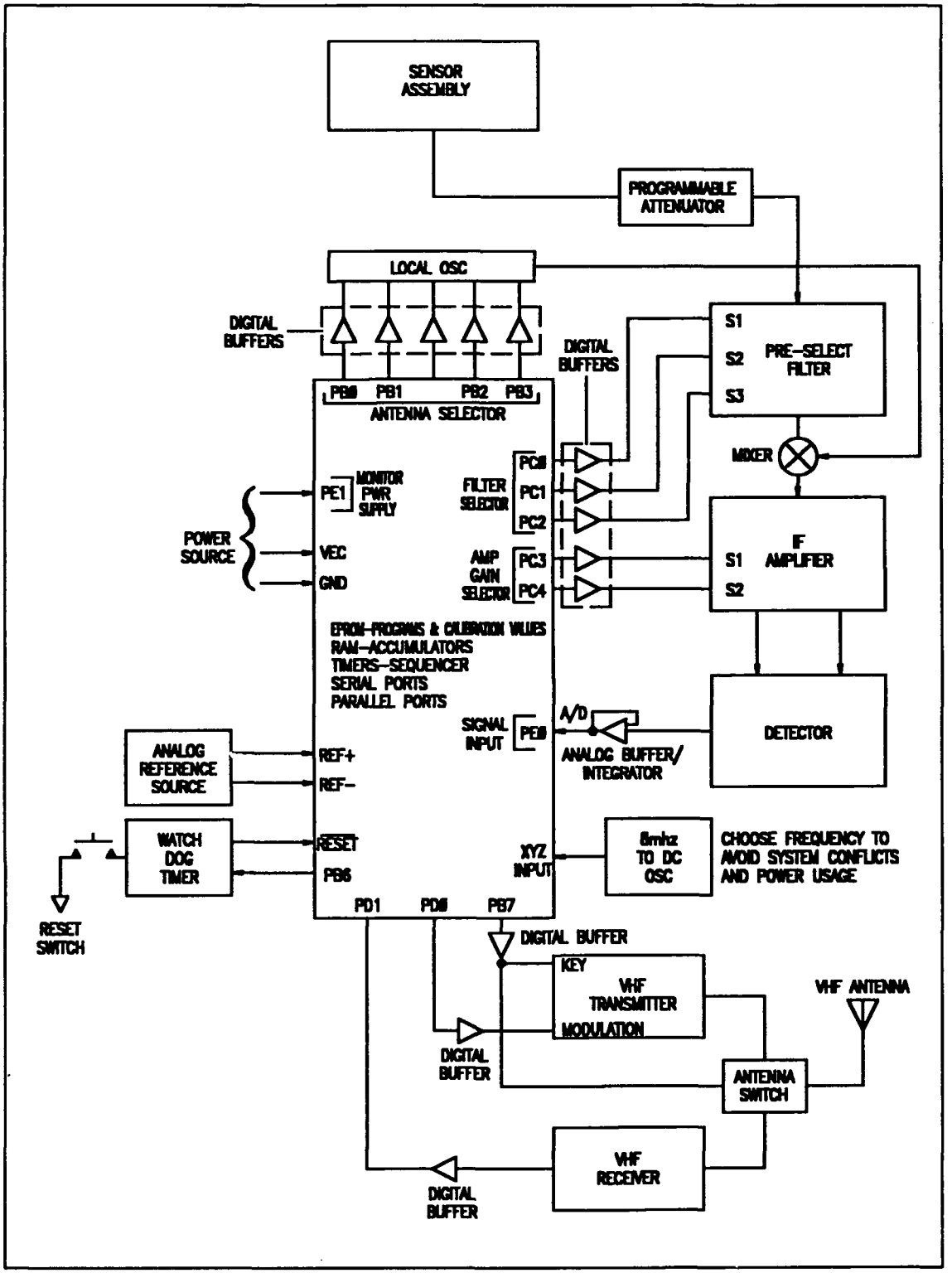

Figure 6-5 Sensor Unit Microprocessor Design

6.5 Power Supply Design

Power can be provided by secondary storage batteries such as gel cells or nicad batteries. Six volt batteries were chosen so that batteries will be inexpensive and easy to obtain. At least eighteen solar cells will be required to attain the voltage of the secondary batteries. It is estimated that 160 cells will be required to charge the batteries in normal conditions. A diagram of the power supply is shown in **Figure 6-6**. The solar charger is directly connected to the battery pack with isolation diodes so that the battery cannot discharge back into the solar cells during periods of darkness. A series regulator will be used to regulate voltage into the computer circuit. The RF equipment will run directly from the battery. Current drain for the microprocessor is about 25 ma. The receiver will take about 100 ma and the transmitter will take at least 0.5 ampere. The duty cycle of the transmitter, fortunately, is very low so that its operation does not appreciably affect the total current drain. The battery, however, must be of sufficient size to supply the peak current load without voltage sag. The battery can be monitored so that a low battery indication is transmitted to the control center. This signal along with others serves as an indicator for maintenance of the unit. The Kwajalein Weather Station was used as a source for data concerning the longest period of cloudy days so that the battery will be properly sized.

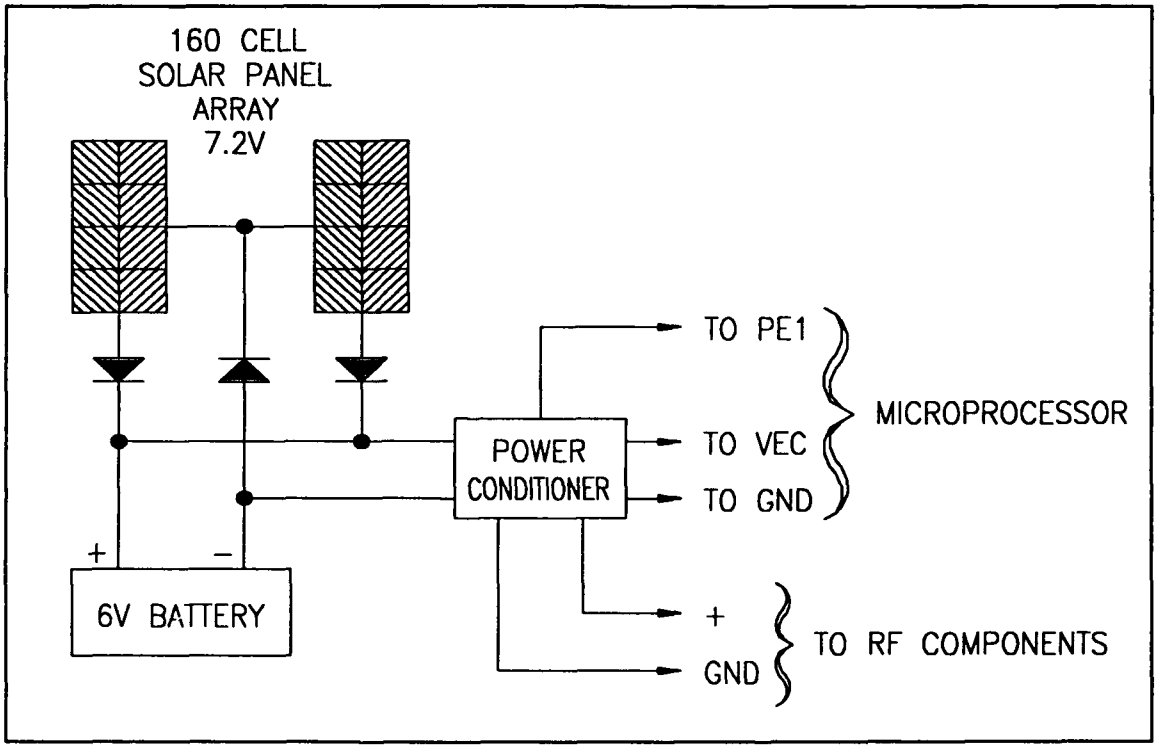

Figure 6-6 Sensor Unit Power System Preliminary Design

6.6 Communications/Telemetry

A telemetry system for communications between the control center and the sensor units was selected in favor of dedicated telephone or other hardware lines. Telemetry is preferred over other means for the following reasons:

1. Allows each unit to act as a stand alone sensor,
2. Allows continued usage of the system if there is a line failure,
3. Allows more flexibility at the site; for instance, fewer buried cables in the site area which can interfere with future construction, and
4. Telemetry is more impervious to natural hazards than buried cable.

In order to use a telemetry system for this purpose, a frequency was carefully chosen so that no RF interference will be introduced to the radar receiving systems. Two hundred megahertz was chosen for this frequency because it is between the VHF and UHF frequency bands of the most sensitive receivers of ALTAIR. This frequency choice was coordinated with the Range and a test was conducted using a surrogate transmitter which was operated at 200 MHz. This transmitter has a 1 watt output and was operated with a 1/4 wave vertical dipole antenna. The second harmonic at 400 MHz was specified to be down 60 dBc.

Testing was completed by Mr. Ron Kuratsu, an Aeromet Engineer, who operates and maintains RF equipment at the Weather Station, Kwajalein. These tests were coordinated and scheduled with Mr. Mike Wyatt, Dyncorp Frequency Analysis Group, and involved ALTAIR receiver and pedestal control personnel.

Tests were conducted on two separate occasions and no RF frequency interference was detected by the ALTAIR operators. A letter depicting the tests is included in Appendix III.

Since 1 watt was arbitrarily chosen for the tests, a link budget was prepared for a 1 watt system. In this budget a link margin of 54.0 dB was calculated. For a system such as this, 54 dB is an overabundance. Another link budget was prepared using 100 milliwatts. In this case, the link margin is 44.0 dB. These calculations show that the 100 milliwatt telemetry system will be more than adequate. Link budgets are included in **Table 6-1**. A rule of thumb requires a +10 dB margin.

A block diagram of the telemetry/communications system is shown in **Figure 6-7**. The control center will act as master and the sensor units will act as slaves. The master is a full duplex station and will issue commands on a separate channel. The slaves can be assigned to several frequency groups depending on the total number of units required. The slaves of a particular frequency group "report in" (serially) on a time scheduled basis which is determined and assigned by the master.

In this way, expensive multiplexers for the slaves are avoided. Also, time is coordinated by the master. The master will be updated daily with Range time and will pass the time to the slaves daily. Since the slaves will be controlled by a microprocessor, time keeping and coordination is a relatively simple task.

Table 6-1 Telemetry

LINK BUDGET 200 MHz		
System	**1watt**	**.1watt**
Tx power	0dBw	-10dBw
Tx Antenna Match	-1	-1
Tx Antenna gain	0	0
Transmission Loss (2 miles)	-90	-90
Rx Antenna gain	0	0
Rx Antenna Match	-1	-1
Boltzmann's Constant	+228.6	+228.6
Rx Noise Temperature (300 Deg. K.)	-24.8	-24.8
Rx Noise Figure	-3	-3
Rx Signal to Noise Ratio	-12	-12
Post Detection BW 19.2 K baud	-42.8	-42.8
Margin	**+54.0**	**+44.0**

6.7 Sensor Unit Calibration

Calibration is an important part of the Aeromet concept for measuring RF hazard energy. Equipment will be provided for calibration in the control center. Overall calibration will be accomplished by placing the sensor unit in a chamber and applying calibration levels of RF energy in the hazard bands required. This test data will be corroborated by use of a Narda Radiation Meter as a control. Software will be used to change the gain constants required for calibration.

The hardware will be tested periodically to see that the circuitry has not degraded over time. There will be a test port where signal levels can be input to the microprocessor

so that the microprocessor can be tested for relative function and accuracy.

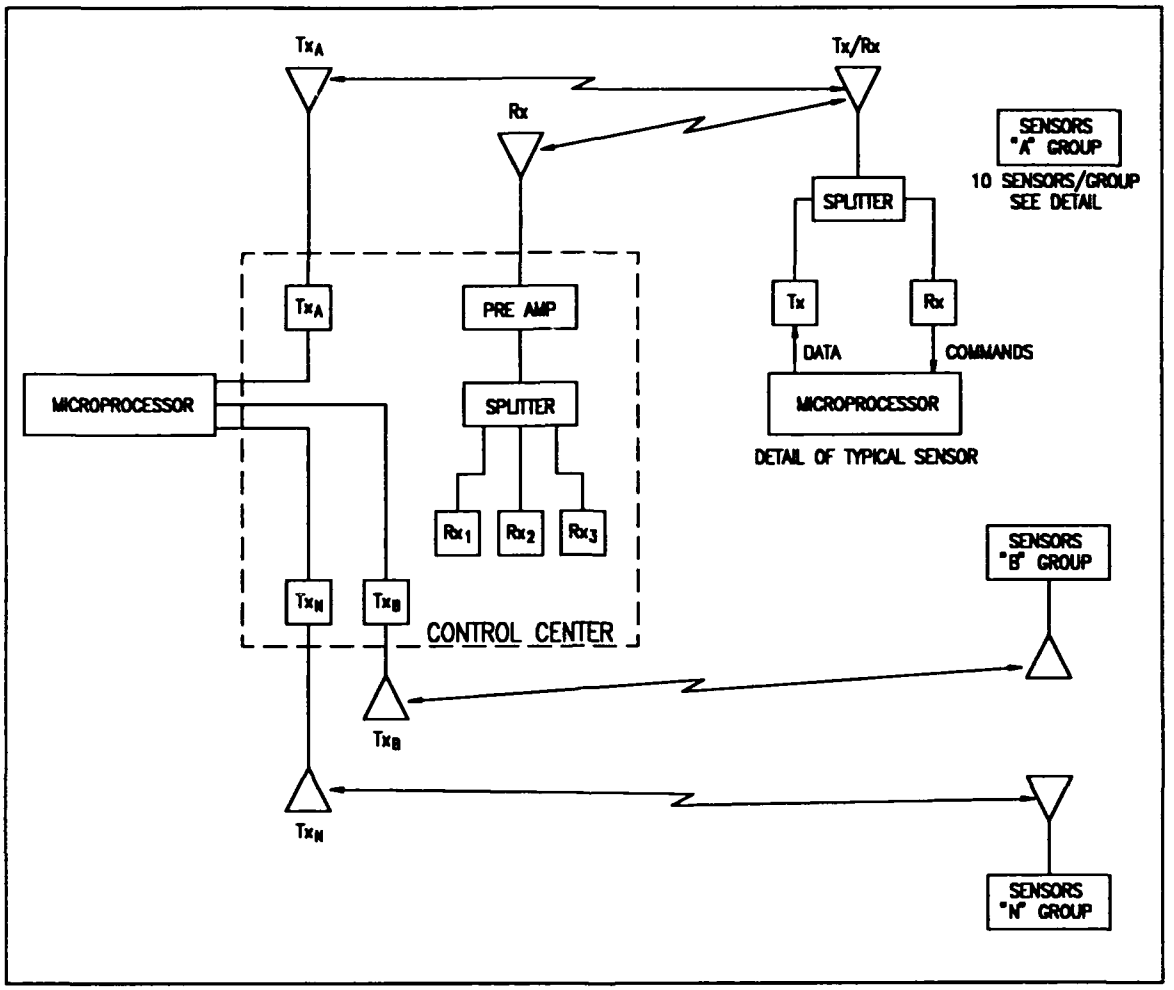

Figure 6-7 Communication/Telemetry System Proposed Design

7. PRELIMINARY DESIGN OF DATA GATHERING SYSTEM

7.1 Preliminary Design of Data Gathering System

In order to design a microprocessor system for use in gathering the telemetered RF hazard data, it is important to define how it is to be used. One way of doing this is to anticipate perceived operational scenarios and perceived control center and remote sensor tasks and design a system to accommodate these scenarios and tasks. Coordination with personnel at USAKA have provided insight that helped to develop the following scenarios.

7.1.1 Operational Scenarios

7.1.1.1 Routine RF Hazard Monitoring

- Operator at control center activates routine RF hazard monitoring software routine.
- Control center polls each remote sensor to send current sensor data at 1 hour intervals.
- Control center stores remote sensor data and tags it "routine".
- Control center displays updated contour maps with selectable working shift variants.

7.1.1.2 RF Hazard Mapping

- Operator at control center activates RF hazard mapping software routine.
- Control center polls each remote sensor to send current sensor data.
- Control center stores remote sensor data and tags it "routine".
- Control center polls each remote sensor to send data at one minute intervals.
- Control center stores remote sensor data and tags it "mapping".

- The control center can produce RF contour maps for spectral energy levels which include :
  1. One minute dosage levels.
  2. Accumulated dosage levels from beginning of test.

7.1.1.3 Mission RF Hazard Monitoring/Warning

- Operator at control center would activate mission RF hazard warning routine.
- Control center would poll each remote station to send current sensor data.
- Control center stores remote sensor data. Tags it as "routine".
- Control center would poll each remote station to send current sensor data every minute.
- Control center stores remote sensor data. Tags it as "mission".
- Control center would produce RF contour dosage level maps for spectral energy levels, one minute dosage levels, and total from start of mission routine activation, dosage levels.
- Alarm signal would be enabled if any regional dosage limits are exceeded.

7.1.2 Control Center and Remote Sensor Tasks

The following is a list of system tasks required to fulfill the operational scenarios listed above.

7.1.2.1 Control Center Tasks

- User Interfaces
  1. Start routine, RF hazard monitoring system.
  2. Start routine, RF hazard mapping system.
  3. Start routine, Mission Warning system.
  4. Menu of available charts for selection.
  5. Analysis of archived data.
- Send commands to remote sensors.

- Store received sensor data.
- Calibration for remote sensors.

7.1.2.2 Remote Sensor Tasks

- Receive control center commands.
- Monitor battery power.
- Review and interpret command center commands.
- Select local oscillator frequency.
- Select RF Band Pass filter.
- Select amplifier gain.
- Sample received signal.
- Adjust frequencies amp gain value for next cycle.
- Sum sampled data into spectral accumulation bucket.
- Switch antenna to/from the communications transmitter and receiver.
- Periodically transmit the sensor data packet to the control center.

7.2 Microprocessor Selection

The MC68HC811E2 is a single-chip microprocessor that utilizes HCMOS[10] technology to provide the low-power characteristics and high noise immunity of CMOS[11], plus the high-speed operation of HMOS[12]. On-chip memory systems include 2,048 bytes of electrically erasable programmable ROM[13] (EEPROM[14]), and

---

10 HCMOS High-Density Complementary Metal-Oxide Semiconductor

11 CMOS Complementary Metal-Oxide Semiconductor

12 HMOS High-Density Metal-Oxide Semiconductor

13 ROM Read Only Memory

14 EEPROM Electrically Erasible Programmable Read Only Memory

256 bytes of static RAM[15]. The HC11 microcomputer also provides highly sophisticated, on-chip peripheral functions, including: an 8 channel A/D[16] converter; 24 digital input/output lines; an SCI[17] subsystem; and an SPI[18] subsystem.

The timer system provides three input capture lines, five output compare lines, and a real time interrupt circuit.

Other features include: a pulse accumulator which can be used to count external events (event counting mode) or measure an external period; a COP[19] watchdog system which helps protect against software failures; a clock monitor system which causes generation of a system reset in case the clock is lost or running too slow; an illegal opcode detection circuit which provides an unmaskable interrupt if an illegal opcode fetch is detected; and two power saving modes, "stop" and "wait". A block diagram of the HC11 is shown in **Figure 7-1**.

Several other types of microprocessors, microcontrollers, and DSPs[20] were considered for this application, but the HC11 appeared to be the best choice for this application.

---

15 RAM Random Access Memory

16 A/D Analog to Digital

17 SCI Serial Communication Interface

18 SPI Serial Peripheral Interface

19 COP Computer Operating Properly

20 DSP Digital Signal Processor

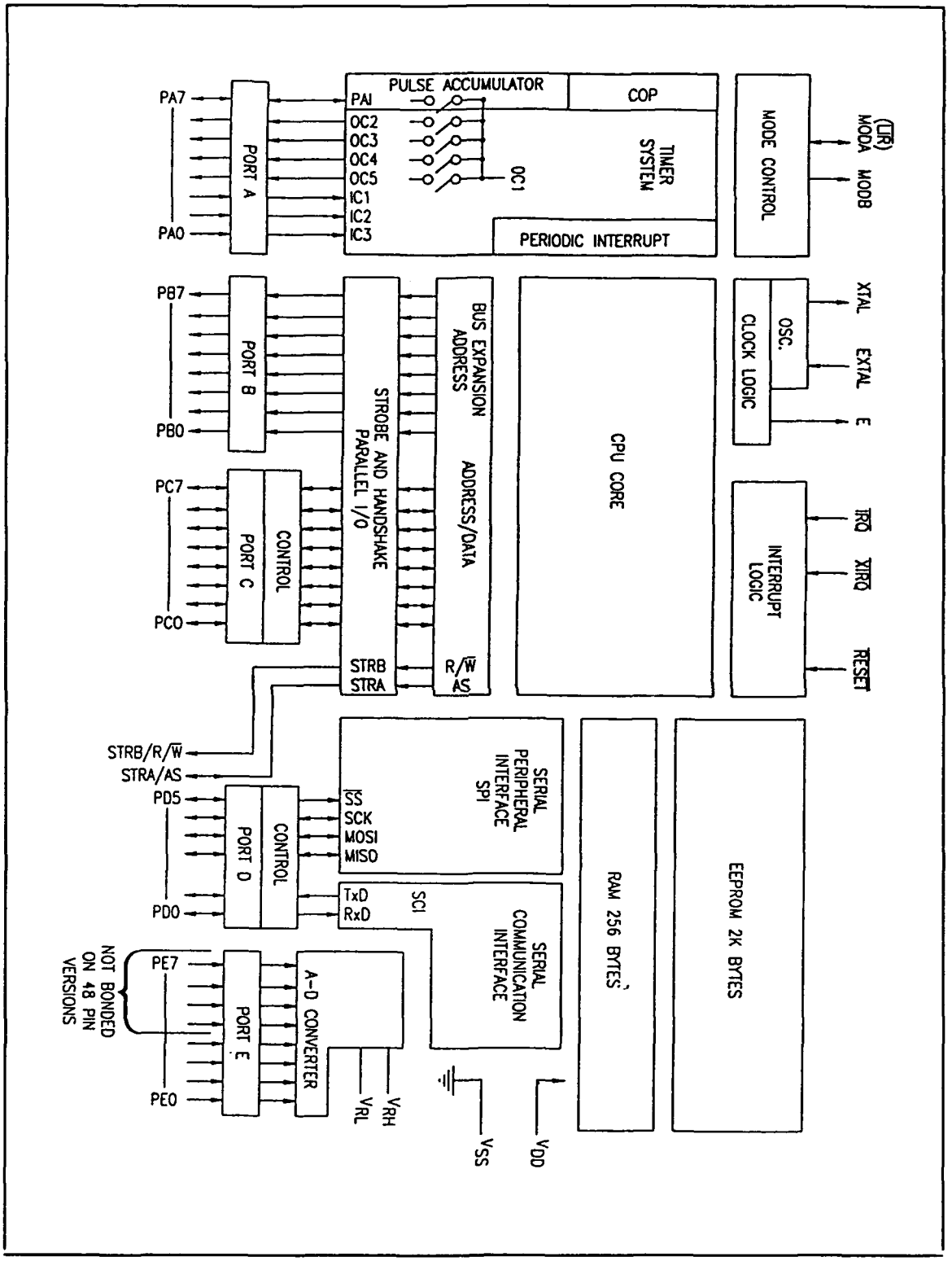

Figure 7-1 Basic HC11 Microprocessor Layout

8. PROPOSED DESIGN OF THE COMMUNICATION SYSTEM

An operating frequency of 200 MHz was chosen for use as a communication channel for the command and control of the sensor units. The same channel will be used for data acquisition. A block diagram of the system is shown in **Figure 6-7**. The system will be designed to operate at 19.2 K baud and FM transmission will be used so as to attain better immunity to RF noise. Aeromet has coordinated the selection and use of this frequency with USAKA Frequency Control and ALTAIR.

A test transmitter was obtained and sent to the USAKA Weather Station. One of the station engineers brought the transmitter to ROI-Namur for interference testing with ALTAIR. This test was at the suggestion of Dr. Burrows. Results of this test indicated that no interference was observed at the ALTAIR site. See **Appendix III.**

An operating frequency of 200MHz was chosen because it is approximately midway between the ALTAIR VHF and UHF bands. Also, the second harmonic (400 MHz) is out of the passband of ALTAIR's UHF band.

The proposed data format for the sensor units is shown in **Table 8-1** and the proposed data format for the control center is shown in **Table 8-2**. The system operates on the principal that the control center is the master and all sensor units are slaves.

Table 8-1 Remote Sensor Data Format

Item	Size	Data Type
Sensor Number	8 Bits	Binary Number
Data Type	8 Bits (Routine Data, Hazard Mapping and Mission Data)	Binary Code
Start Time of Sample	24 Bits	6 BCD Digits
Start Data of Sample	24 Bits	6 BCD Digits
Stop Time of Sample	24 Bits	6 BCD Digits
Stop Date of Sample	24 Bits	6 BCD Digits
Frequency #1 Accumulated Value	16 Bits: 1) 8 Bit Binary Gain Multiplier; 2) 8 Bit Binary A/D Value	2 Binary Numbers
Frequency #2 Accumulated Value	16 Bits	2 Binary Numbers
Frequency #3 Accumulated Value	16 Bits	2 Binary Numbers
Frequency #4 Accumulated Value	16 Bits	2 Binary Numbers
Frequency #5 Accumulated Value	16 Bits	2 Binary Numbers
Cyclic Redundancy Check	16 Bits	Binary Number
Total Packet Size	**26 Bytes**	

Table 8-2 Control Center Data Format

Item	Size	Data Type
Sensor Number	8 Bits	Binary Number
Data Type (Routine Data, Hazard Mapping & Mission Data)	8 Bits	Binary Code
Sensor Latitude	28 Bits	7 BCD Digits
Sensor Longitude	24 Bits	6 BCD Digits
Sensor Elevation	12 Bits	3 BCD Digits
Radar Number	8 Bits	Binary Number
Radar Azimuth	12 Bits	3 BCD Digits
Radar Elevation	8 Bits	2 BCD Digits
Radar Power Level	20 Bits	Binary Number
Start Time of Sample	24 Bits	6 BCD Digits
Start Date of Sample	24 Bits	6 BCD Digits
Stop Time of Sample	24 Bits	6 BCD Digits
Stop Date of Sample	24 Bits	6 BCD Digits
Frequency #1 Accumulated Value	16 Bits 1) 8 Bit Binary Gain Multiplier 2) 8 Bit A/D Value	2 Binary Numbers
Frequency #2 Accumulated Value	16 Bits	2 Binary Numbers
Frequency #3 Accumulated Value	16 Bits	2 Binary Numbers
Frequency #4 Accumulated Value	16 Bits	2 Binary Numbers
Frequency #5 Accumulated Value	16 Bits	2 Binary Numbers
Storage Requirements Per Sensor Sample	**38 Bytes**	

9. PROPOSED DESIGN OF THE CONTROL CENTER

The control center is the heart of the RF hazard measurement system. It controls the mode of data acquisition, allows interactive operation with the radars, stores the acquired data, and allows display or hardcopy of current or archived data.

A system block diagram of the control center is shown in **Figure 9-1**. A computer will be used as the main building block. It can be either a PC or VME based system. PC's are inexpensive, reliable, and easy to operate. Also, a PC system will be easy to upgrade.

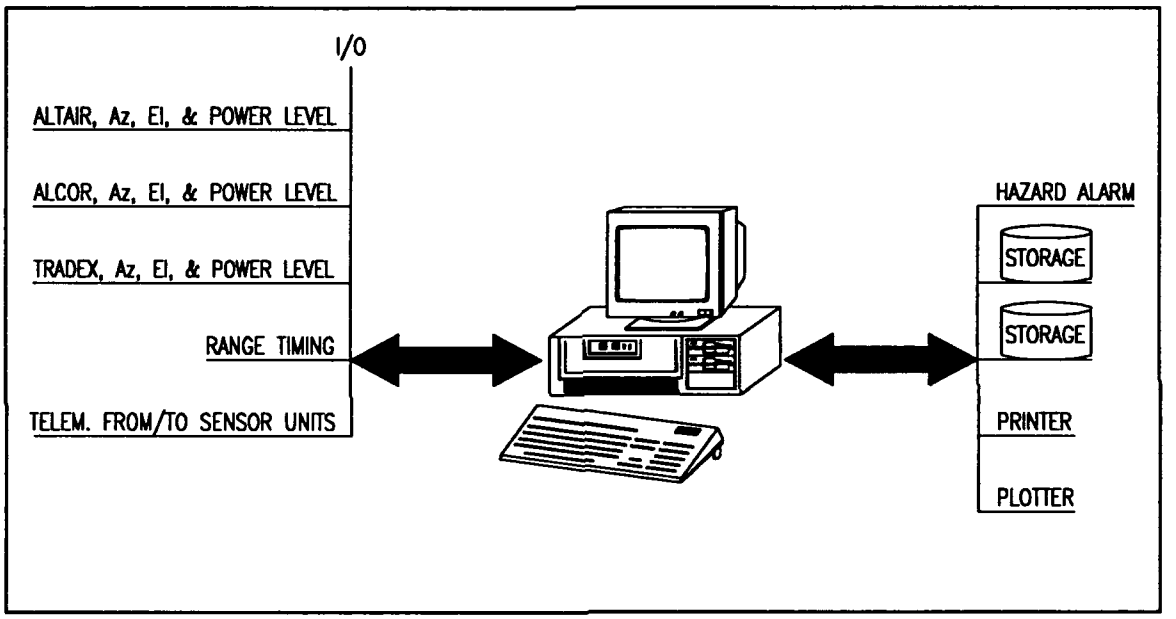

Figure 9-1 Control Center System Block Diagram

Aeromet has, however, developed a VME data acquisition system based on the Motorola 68020 microprocessor. Part of a Phase II effort will be to choose a microprocessor which is best suited for the job. The Aeromet VME[21] system has routines already written that allow acquisition, various technical displays and a system for storing data on a write once read many (WORM[22]) optical disk drive unit. Since software has been developed for this system, implementation of the system may be less expensive than a PC based system. Only one optical disk is expected to be used per year.

---

21 VME Versa-Module Euro

22 WORM Write Once Read Many

The location of the control center is not important as long as it is on the island where the sensors are located so that RF communication can be used to program the sensor units and gather the data. An artist's conception of the control center computer station is shown in **Figure 9-2.**

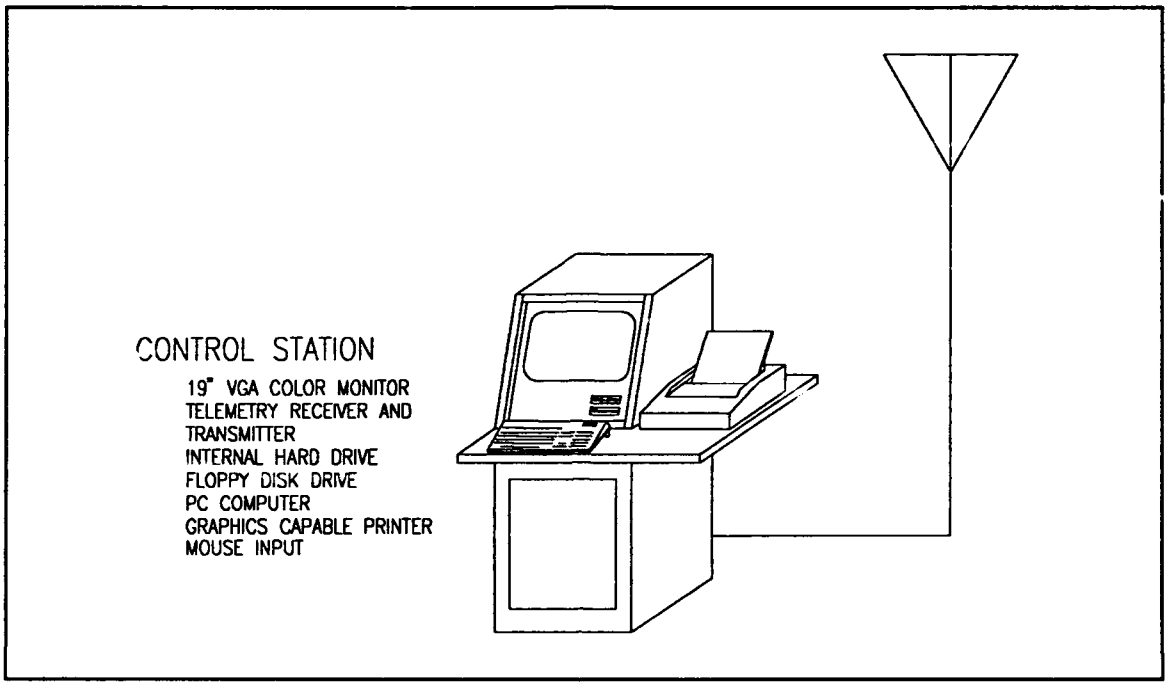

Figure 9-2 Control Center Physical Layout

The control center will not need to be manned full time as it will normally be in routine mode which is automatic. It is expected that for special modes of operation such as interactive positioning of a particular radar or mission mode, the center will require manned operation. Additionally, if special data is to be retrieved and integrated for a particular sensor site, manned operation is anticipated.

When a particular source is identified as exceeding RF hazard limits, a signal will be sent to that source. Details of how this will be accomplished will be addressed in a Phase II proposal

From the block diagram shown in **Figure 9-1**, it can be seen that the control center and associated microprocessor contains electronic circuitry and equipment to provide the following functions:

- I/O radars, azimuth, elevation, active/inactive, power level.
- I/O, range time.
- I/O, RF link to sensor units, XMIT and RX.

- I/O, remote monitors, for radar sites.
- I/O, hazard alert or alarm.
- Display.
- Process.
- Control.
- Store.
- Archive.
- Retrieve.
- Integrate and
- Map

There are a great number of displays and plots that are possible by calling the stored routines in the control center microprocessor. Examples of some of these displays are shown in **Figure 9-3**.

The resolution of the displayed data will determine the number of sensor units that are required. Phase II work will include a statistical analysis to determine the optimal number of sensor units that are required.

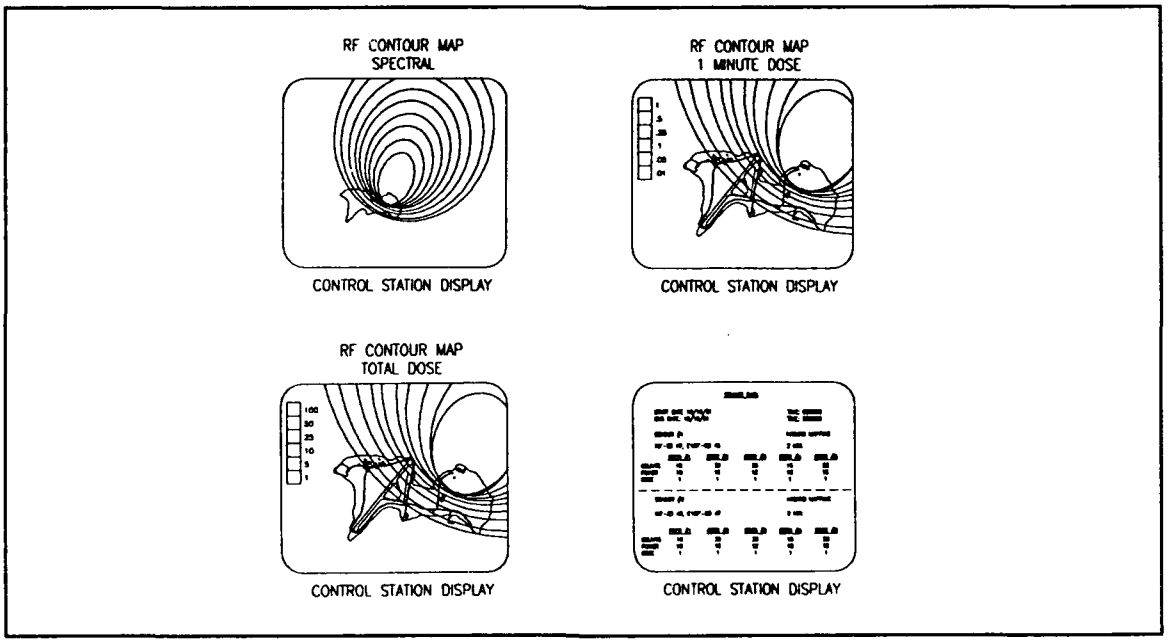

Figure 9-3 Control Center Proposed Displays/Plots

10. CONCLUSIONS

The research and testing that was completed during this Phase I work indicates that the concept for this radiation monitor is sound. All of the Phase I objectives were satisfied and a Phase II proposal can be made from the data contained in this report. An automated system such as described herein will be presented and costed in the format of a Phase II proposal. The system will contain one control center and as many sensor units as required for a hardware proof of system concept.

Ideally, the RF hazard monitoring system should be operated under the eyes of Range Safety, but CRT monitors should be provided for controllers of each radar so that interactive-graphic display and control of the radar can be accomplished without the aid of a Range safety control officer.

Use of the system will address the following hazards that may exist at the radar site:

1. PEAK EXPOSURE. RF radiation levels are not checked or monitored during mission support when radar power is usually maximum and antenna position can be close to the horizon.
2. ACCUMULATIVE EXPOSURE. Since radiation poisoning is accumulative in the human body, radiation levels need to be accumulated and monitored over time, especially near the housing areas because personal exposure levels could become high even when the antennas are pointing in the opposite direction i.e., Front to back ratios for most parabolic reflectors do not usually exceed 50 dB.

Personal peak exposure can be eliminated and workers could be rotated in order to reduce accumulative exposure.

APPENDIX I

Feasibility Test Results
Tri-Axis Elements

Tulsa

DATA SHEET

CHART #: 3.1

ELEMENT TYPE: Tri-axis Dipole

FIELD TYPE: E

SEPARATION: 30 Ft. 0 In.

Reference Level: -19.0 dB
Test Element Level: -41.5 dB

Loss/Gain: 22.5 dB

Horiz. Plane Rotation:
Max. Level: -41 dB
Min. Level: -41.5 dB

Spread: 0.5 dB

Vert. Plane Rotation:
Max. Level: -41 dB
Min. Level: -41.5 dB

Spread: 0.5 dB

Comments: VHF, 162 MHz

Date: July 9, 1991

Technician: [signature]

DATA SHEET

CHART #: 3.2

ELEMENT TYPE: Tri-axis coil

FIELD TYPE: H

SEPARATION: N/A Ft. ____ In.

Reference Level: -55 dB
Test Element Level: -70 dB

Loss/Gain: 15 dB

Horiz. Plane Rotation:
Max. Level: -70.3 dB
Min. Level: -70 dB

Spread: 0.3 dB

Vert. Plane Rotation:
Max. Level: -70.5 dB
Min. Level: -70 dB

Spread: 0.5 dB

Comments: VHF, 162 MHz
E Field rejection = -31 dB

Date: July 9, 1991

Technician: DB

DATA SHEET

CHART #: 3.3

ELEMENT TYPE: Tri-axis Dipole

FIELD TYPE: E

SEPARATION: 30 Ft. 0 In.

Reference Level: -26.83 dB
Test Element Level: -37.00 dB

Loss/Gain: 10.17 dB

Horiz. Plane Rotation:
Max. Level: -37.1 dB
Min. Level: -37.4 dB

Spread: 0.3 dB

Vert. Plane Rotation:
Max. Level: -37.0 dB
Min. Level: -37.2 dB

Spread: 0.2 dB

Comments: UHF, 422 MHz

H field rejection = -12 dB, H Field radiation
N field rejection in N field = -20 dB

Date: July 10, 1991

Technician: [illegible]

DATA SHEET

CHART #: 3.4

ELEMENT TYPE: Tri-axis Coil

FIELD TYPE: H

SEPARATION: N/A Ft. ~ In.

Reference Level: -60.5 dB
Test Element Level: -15.5 dB

Loss/Gain: 45 dB

Horiz. Plane Rotation:
Max. Level: -15.5 dB
Min. Level: -16.1 dB

Spread: -0.6 dB

Vert. Plane Rotation:
Max. Level: -15.5 dB
Min. Level: -16.0 dB

Spread: 0.5 dB

Comments: UHF, All Axis
E field injection = -24.5 dB

Date: July 10, 1991

Technician: [illegible]

DATA SHEET

CHART #: 3, 5

ELEMENT TYPE: Tri-axis Dipole

FIELD TYPE: E

SEPARATION: 30 Ft. 0 In.

Reference Level: -39.17 dB
Test Element Level: -40.0 dB

Loss/Gain: 1.83 dB

Horiz. Plane Rotation:
Max. Level: -40.0 dB
Min. Level: -40.4 dB

Spread: 0.4 dB

Vert. Plane Rotation:
Max. Level: -40.0 dB
Min. Level: -40.5 dB

Spread: 0.5 dB

Comments: L-Band 1320 MHz
H Field Rejection = 8dB

Date: July 10, 1991

Technician: [signature]

DATA SHEET

CHART #: 3.6

ELEMENT TYPE: Tri-axis Coil

FIELD TYPE: H

SEPARATION: N/A Ft. ____ In.

Reference Level: -59 dB
Test Element Level : -14 dB

Loss/Gain: 45 dB

Horiz. Plane Rotation:
Max. Level: -14.0 dB
Min. Level: -14.72 dB

Spread: 0.72 dB

Vert. Plane Rotation:
Max. Level: -14 dB
Min. Level: -14 dB

Spread: 0 dB

Comments: L-Band

No rejection to E-Field.

Date: July 10, 1991

Technician: [signature]

DATA SHEET

CHART #: 3.8

ELEMENT TYPE: Tri-axis Dipole

FIELD TYPE: E

SEPARATION: 30 Ft. 0 In.

Reference Level: -54 dB
Test Element Level: -48 dB

Loss/Gain: 6 dB

Horiz. Plane Rotation:
Max. Level: -48.0 dB
Min. Level: -48.6 dB

Spread: 0.6 dB

Vert. Plane Rotation:
Max. Level: -48.0 dB
Min. Level: -48.4 dB

Spread: 0.4 dB

Comments: S-Band, 2100 MHz
H-Field rejection = 17 dB

Date: July 11, 1991

Technician: [illegible]

DATA SHEET

CHART #: 3,9

ELEMENT TYPE: Tri-axis Coil

FIELD TYPE: H

SEPARATION: N/A Ft. _____ In.

Reference Level: -62 dB
Test Element Level: -12,67 dB

Loss/Gain: 49,33 dB

Horiz. Plane Rotation:
Max. Level: -12,67 dB
Min. Level: -13,18 dB

Spread: 0,51 dB

Vert. Plane Rotation:
Max. Level: -12,67 dB
Min. Level: -13,20 dB

Spread: 0,53 dB

Comments: S-Band, 2100 mHz
E-Field Rejection = 0 dB

Date: July 11, 1991

Technician: [signature]

DATA SHEET

CHART #: 3.11

ELEMENT TYPE: Tri-axis Dipole

FIELD TYPE: E

SEPARATION: 30 Ft. 0 In.

Reference Level: _____ dB
Test Element Level : _____ dB

Loss/Gain: _____ dB

Horiz. Plane Rotation:
Max. Level: _____ dB
Min. Level: _____ dB

Spread: _____ dB

Vert. Plane Rotation:
Max. Level: _____ dB
Min. Level: _____ dB

Spread: _____ dB

Comments: This test could not be completed due to equipment (limited range of test equipment) C-band on 4600 mhz

Date: July 12, 1991

Technician: DB

DATA SHEET

CHART #: 3012

ELEMENT TYPE: Tri-axis Coil

FIELD TYPE: H

SEPARATION: _____ Ft. _____ In.

Reference Level: _____ dB
Test Element Level : _____ dB

Loss/Gain: _____ dB

Horiz. Plane Rotation:
Max. Level: _____ dB
Min. Level: _____ dB

Spread: _____ dB

Vert. Plane Rotation:
Max. Level: _____ dB
Min. Level: _____ dB

Spread: _____ dB

Comments: This test could not be completed due to equipment (limited range of test equipment) C-Band = 5.600 MHz

Date: July 12, 1991

Technician: [signature]

APPENDIX II

Feasibility Test Results
Micro-Strip Antenna

Tulsa

DATA SHEET

CHART #: 3.7

ELEMENT TYPE: ½ λ Dipole to MICRO-STRIP

FIELD TYPE: Electric — HORIZONTAL POL./VERT. POL.

SEPARATION: 20 Ft. 0 In.

Reference Level: -41.60 dB
Test Element Level: -56.00 dB

Loss/Gain: 14.4 dB

Horiz. Plane Rotation:
Max. Level: -56.00 dB
Min. Level: -65.50 dB

Spread: 9.5 dB

Vert. Plane Rotation:
Max. Level: -59.5 dB
Min. Level: -60.3 dB

Spread: .8 dB

Comments: 2630 MHZ

Poor edge response

Date: 7-11-91

Technician: Dale Lawson / John Lofton

DATA SHEET

CHART #: 3.10

ELEMENT TYPE: ½ λ Dipole to Microstrip

FIELD TYPE: E-Field

SEPARATION: 20 Ft. 0 In.

Reference Level: -48.2 dB
Test Element Level: -63.7 dB

Loss/Gain: 15.5 dB

Horiz. Plane Rotation:
Max. Level: -69.5 dB
Min. Level: -71.5 dB

Spread: 2.0 dB

Vert. Plane Rotation:
Max. Level: 67.3 dB
Min. Level: 69.8 dB

Spread: 2.5 dB

Comments: 5656 MHz

Poor side on response

Date: 7/11/91

Technician: DG

APPENDIX III

Feasibility Test Results
Frequency Selection
Communications/Telemetry System

Roi-Namur

aeromet MEMO

To: Dave Brown

From: R.H. Kuratsu

Date: October 2, 1991

Subject: Roi-Namur interference test..

Scheduled the RF testing with KREMS and with the assistance of Mr. Mike Wyatt, Dyncorp Frequency Analysis Group, proceeded testing transmitter. This involved ALTAIR receiver and pedestal control personnel. Azimuth and Elevation scans were initiated and no interference was witnessed by ALTAIR personnel. UHF and VHF frequencies were monitored. Mr. Wyatt verified transmitter was being cycled on and off utilizing a portable power monitor. ALTAIR was satisfied that no interference was being generated by the test transmitter.

APPENDIX IV

Feasibility Test Results
Tri-Axis Coil Test

DATA SHEET

CHART #: 13

ELEMENT TYPE: Tri-axis coil

FIELD TYPE: H

SEPARATION: — Ft. — In.

Reference Level: +15 dBm
Test Element Level: -12 dBm

Loss/Gain: 13 dB

Horiz. Plane Rotation:
Max. Level: -12 dBm
Min. Level: -12.2 dBm

Spread: 0.2 dB

Vert. Plane Rotation:
Max. Level: -12.1 dBm
Min. Level: -12.2 dBm

Spread: 0.1 dB

Comments:
The sensor was placed inside a coil where a known field was induced at 16.2 MHz
The sensor output varied less than ± 0.2 dB throughout the rotations
Theoretical value = -12.07 dBm

Date: 7/1/91

Technician: DB

REFERENCES

Jasik, Henry, 1961: *Antenna Engineering Handbook*, USA, McGraw-Hill.

Lee, Kai Fong, 1984: *Principles of Antenna Theory*, New York, John Wiley & Sons

Skolnik, Merrill I., 1990: *Radar Handbook*, USA, McGraw-Hill.

Edwards, T.C., 1981: *Foundations of Microstrip Circuit Design*, John Wiley & Sons.

Authors, Compiled, 1988: *ARRL Antenna Handbook*, USA, American Radio Relay League.

Bhartia, P. and Bahl, I. J., October 1982: *Frequency Style Microstrip Antenna*, Microwave Journal.